Distribution Agreement

In presenting this thesis or dissertation as a partial fulfillment of the requirements for an advanced degree from Emory University, I hereby grant to Emory University and its agents the non-exclusive license to archive, make accessible, and display my thesis or dissertation in whole or in part in all forms of media, now or hereafter known, including display on the world wide web. I understand that I may select some access restrictions as part of the online submission of this thesis or dissertation. I retain all ownership rights to the copyright of the thesis or dissertation. I also retain the right to use in future works (such as articles or books) all or part of this thesis or dissertation.

Signature:

_____ _____

Mackenzie Prichard

Cis-regulatory methylation of the *VIP* gene in the white-throated sparrow (*Zonotrichia albicollis*)

By

Mackenzie Prichard

Master of Arts

Psychology: Neuroscience & Animal Behavior

_____

Donna Maney Ph.D.
Advisor

_____

Sherryl Goodman, Ph.D.
Committee Member

_____

Aubrey Kelly, Ph.D.
Committee Member

Accepted:

_____

Lisa A. Tedesco, Ph.D.
Dean of the James T. Laney School of Graduate Studies

_____

Date

Cis-regulatory methylation of the *VIP* gene in the white-throated sparrow (*Zonotrichia albicollis*)

By

Mackenzie R. Prichard

B.S., University of Montana

Adviser: Donna L. Maney, Ph.D.

An abstract of

A thesis submitted to the Faculty of the

James T. Laney School of Graduate Studies of Emory University

in partial fulfillment of the requirements for the degree of

Master of Arts

in Psychology

2021

Abstract

Cis-regulatory methylation of the *VIP* gene in the white-throated sparrow (*Zonotrichia albicollis*)

By Mackenzie Prichard

Pathways between genotype and phenotype, especially a behavioral phenotype, are complicated by many levels of biological organization, making direct connections difficult. Animal models with clear connections between genotype and behavioral phenotype are needed. One such model is the white-throated sparrow. In this species, a rearrangement of the second chromosome is linked with territorial aggression. Birds with a copy of the rearrangement are more aggressive than those without it. The rearrangement has captured the gene *VIP*, which encodes vasoactive intestinal peptide, a neuromodulator known to be causal for aggression in other songbirds. *VIP* expression is higher in the anterior hypothalamus of birds with the rearrangement than those without it and expression of *VIP* in this region predicts the level of territorial aggression regardless of genotype. Thus, hypothalamic *VIP* is a strong candidate to mediate this behavioral polymorphism. For example, due to differentiation between the standard and rearranged chromosomes, there are two distinct alleles of *VIP*. The two alleles may be transcribed at different levels, leading to morph differences in expression. Here, we aimed to identify epigenetic mechanisms that could contribute to such allelic imbalance. We extracted and bisulfite-converted DNA from samples of the hypothalamus in wild-caught adults and nestlings and used high-throughput sequencing to measure DNA methylation of a region 1.2kb upstream of the *VIP* start site. We found that the methylation of this region was lower on the allele inside the rearrangement than on the alternative allele. In addition, methylation differed between the alleles at specific sites within this putative cis-regulatory element. This work represents an initial step toward understanding how epigenetic differentiation inside chromosomal inversions leads to the development of alternative behavioral phenotypes.

Cis-regulatory methylation of the *VIP* gene in the white-throated sparrow (*Zonotrichia albicollis*)

By

Mackenzie R. Prichard

B.S., University of Montana

Adviser: Donna L. Maney, Ph.D.

A thesis submitted to the Faculty of the

James T. Laney School of Graduate Studies of Emory University

in partial fulfillment of the requirements for the degree of

Master of Arts

in Psychology

2021

Acknowledgement

This project came to fruition through the collaborative efforts of several people over several years. The birds that were collected for this study were captured by Dr. Brent Horton and Dr. Wendy Zinzow-Kramer. Tissue processing and sequencing library prep were conducted by Dr. Wendy Zinzow-Kramer, Dr. Kathleen Grogan, Dr. Jennifer Merritt, and Jessia Root. I processed the sequencing data, conducted the statistical analyses, prepared all graphs and tables, and wrote the paper. The parts of the project that were conducted by multiple people are written in plural first person (i.e., "We conducted") and the parts of this project that were conducted by myself are written in singular first person (i.e., "I found"). Dr. Donna Maney supervised the project from start to finish and provided advice, support, and guidance at every step of this project, which made this project successful.

This work was also conducted on the stolen land of many Indigenous peoples who were and are still displaced by colonizers. Most of the lab work, data analysis, and writing was conducted on Muscogee Creek land. The white-throated sparrow population in this study was from Abenaki / Abénaquis, Penobscot and Wabanaki Confederacy land. Some sequencing was conducted on Shakori land. This project was also conducted through infrastructure that was built in part by enslaved African people.

I want to personally thank my friends, family, and teammates that have been there to support me throughout this process. I finished this project during a truly intense period in history and I couldn't have done it without you.

Table of Contents

Introduction

The genetic basis of behavior is one of the more complicated and challenging topics of research because of the multiply determined nature of behavioral phenotypes. Behaviors may depend on intrinsic factors, such as the stage of development, and extrinsic factors, such as social context. The changeability of behavior is critical for survival and reproduction in every animal and is why behavior is so interesting from an evolutionary perspective. To understand how behavior evolves, we must understand how behaviors are inherited and rooted in genetics. Pathways between the genome and any phenotype, but especially pathways between genes and behaviors, are complicated by many levels of biological organization, which makes direct connections between the two endpoints impossible. However, new strategies for detecting genetic mechanisms that regulate gene expression are helping to connect the dots between genes and behavior.

Genetic mechanisms of behavior have been studied primarily in lab-reared model organisms such as mice, rats (Manger et al., 2008), and some invertebrates. Despite this bias in the species represented in the literature, wild and diverse model organisms are invaluable for establishing structure-function relationships between physiology and behavior (Bullock, 1984; Thompson, 2020). For instance, an organism's natural habitat provides evolutionary relevant contexts for quantifying behavioral responses, which is impossible for models such as mice and rats that have been inbred in captivity for countless generations. Historically, strategically selected natural model organisms have been critical for many fundamental discoveries in neurobiology (Keifer & Summers, 2016).

One such strategically selected model organism is the white-throated sparrow (*Zonotrichia albicollis*; Maney, 2008; Maney et al., 2020). In this species, half of the individuals

of any given population have one copy of chromosome two that contains a series of nested inversions, hereafter referred to as ZAL2^{m}, and one copy of this chromosome without the inversions, herein ZAL2 (Thorneycroft, 1975). The other half of the population comprises birds that are homozygous for ZAL2, and birds that are homozygous for the ZAL2^{m} arrangement are exceedingly rare (Horton et al., 2013; Thorneycroft, 1975). ZAL2 homozygotes have duller head plumage than the heterozygotes, which have a bold, bright pattern on their throat and crown. Their plumage patterns have earned them the respective names of tan-striped (TS) and white-striped (WS) (Figure 1; Falls & Kopachena, 2020; Thorneycroft, 1975). Both morphs are equally represented in both sexes, and most breeding pairs consist of one bird of each morph (Falls & Kopachena, 2020; Lowther et al., 1961). In other words, breeding pairs are almost always either WS female / TS male or TS female / WS male, which is why this species is sometimes called the bird with four sexes (Campagna, 2016). WS male / WS female breeding pairs are highly uncommon (Thorneycroft, 1975), which has left ZAL2^{m} in a near-constant state of heterozygosity. For this reason, the ZAL2/2^{m} system is sometimes compared to sex chromosomes (Joron & Whibley, 2011); the mammalian Y and the avian W chromosomes are in a similar, but perhaps more severe, state of perpetual heterozygosity (Tuttle et al., 2016).

The ZAL2/2^{m} rearrangement is responsible for more than just plumage coloration. We have known for many years that the ZAL2^{m} rearrangement affects social behaviors, including aggression and parental behavior (Kopachena & Falls, 1993a; Kopachena & Falls, 1993b). WS birds are more territorially aggressive than TS birds of the same sex, and TS birds are more parental than WS birds of the same sex (Horton et al., 2012; Kopachena & Falls, 1993b). The aggregate effects of the behavioral differences between the morphs have thus resulted in alternative reproductive strategies (Tuttle, 2003). This polymorphism in breeding behavior,

resulting from an underlying genetic polymorphism, makes the white-throated sparrow an ideal model for investigating molecular pathways between the genome and behavior.

One gene within the ZAL2/2^{m} rearrangement is vasoactive intestinal peptide (*VIP*), which is known to affect aggression and thus could contribute to the divergence of aggressive behavior between the morphs. *VIP* is expressed in nearly every brain region associated with social behavior in multiple avian species, including chickens (*Gallus gallus*; Kuenzel et al., 1997), blue tits (*Cyanistes coeruleus*; Montagnese et al., 2015), field sparrows (*Spizella pusilla*), and song sparrows (*Melospiza melodia*; Goodson, 1998; Goodson et al., 2012b). One function of *VIP* in the brain is to modulate social behaviors, including aggression (Kingsbury, 2015; Kingsbury & Wilson, 2016). In the anterior hypothalamus (AH), *VIP* expression correlates with aggressive behaviors in field and song sparrows (Goodson, 1998; Goodson et al., 2012b). Goodson and colleagues (2012a) found a causal effect of *VIP* expression in the AH on aggressive behavior in violet-eared waxbills (*Uraeginthus granatina*). They treated birds with antisense oligonucleotides via cannulae aimed at the AH to knock down *VIP* expression in that region. The knockdown of *VIP* expression resulted in reduced aggression in this and another species, the zebra finch (*Taeniopygia guttata*) (Goodson et al., 2012a). Knocking down *VIP* expression in the AH did not affect other behaviors, such as affiliative or anxiety-like behaviors (Goodson et al., 2012a), providing evidence that *VIP* expression in the AH is causal for aggressive behavior specifically.

Our lab has demonstrated morph differences in the expression of *VIP* in the AH of white-throated sparrows. We used *in situ* hybridization to measure *VIP* expression in the AH of free-living, behaviorally characterized birds (Horton et al., 2020). We found that during the peak of territoriality during the breeding season, *VIP* was expressed at higher levels in the AH of WS

birds than TS birds. Furthermore, we found that *VIP* expression in the same region correlated with aggressive singing rates in both morphs and sexes (Horton et al., 2020). This finding is consistent with the known effect of VIP on aggression in other songbirds (Goodson et al., 2012a) and the relatively more aggressive phenotype of WS birds. Altogether, this evidence points to *VIP* expression as a potential molecular mechanism driving the evolution of the behavioral polymorphism in aggression in this species. However, we have yet to determine whether or how the chromosomal rearrangement mediates the morph difference in expression of *VIP*.

The isolation of ZAL2^{m} in WS birds has led to an accumulation of single nucleotide polymorphisms (SNPs) and insertion/deletion polymorphisms (INDELs) within genes captured by the rearrangement (Davis et al., 2011; Huynh et al., 2011; Sun et al., 2018;). Because the *VIP* gene falls within the ZAL2/2^{m} rearrangement, one explanation for morph differences in expression might be genetic variation between the ZAL2 and ZAL2^{m} alleles of this gene. Notably, there are no changes to the protein-coding sequence between the ZAL2 allele of *VIP* (*VIP*^{2}) and the ZAL2^{m} allele (*VIP*^{2m}) (Sun et al., 2018). However, there are many SNPs and INDELs in *VIP* directly upstream of the transcription start site (Figure 2; Sun et al., 2018). This region is a putative *VIP cis*-regulatory element (CRE), or a genetic sequence that affects the expression of nearby genes. This genetic variation could cause *VIP*^{2} and *VIP*^{2m} to be expressed at different levels, that is, it could contribute to allelic imbalance in *VIP* expression. If there is allelic imbalance such that *VIP*^{2m} is overexpressed relative to *VIP*^{2} then, because TS birds do not have a copy of *VIP*^{2m}, the extra expression of that allele in WS birds could result in higher total *VIP* expression in that morph.

Allelic imbalance in *VIP* expression could be caused by genetic or epigenetic variation between ZAL2/2^{m} in this region. Here, I focus on variation in the methylation of CG

dinucleotides (herein CpGs). Methylation affects transcription factor binding (Heberle & Bardet, 2019) and is vital for tissue-specific regulation of gene expression (Mendizabal & Yi, 2016; Suzuki & Bird, 2008). Methylation is most commonly, but not always, associated with inhibited expression (Eden & Cedar et al., 1994; Mamrut et al., 2013). Using whole-genome bisulfite sequencing in white-throated sparrows, Sun and colleagues (2020) found that most CpGs inside the ZAL2/2^{m} rearrangement were equally likely to be hypo- or hypermethylated on ZAL2 relative to ZAL2^{m}. However, they found that some CpGs were extremely hypomethylated on ZAL2^{m}, suggesting a that ZAL2^{m} is less methylated overall. They also found evidence that the degree of differential methylation between alleles was negatively associated with the degree of differential expression. Altogether, these results are consistent with the hypothesis presented here that epigenetic variation in the *VIP* CRE may contribute to overexpression of *VIP^{2m}* due to hypomethylation on this allele.

In this study, I used next-generation sequencing to answer two central questions about the methylation of *VIP* in a hypothalamic tissue sample containing the AH from white-throated sparrows. First, is there differential methylation between the alleles of the *VIP* CRE? Because *VIP* expression in the AH is higher in WS than TS birds (Horton et al., 2020), I predicted that *VIP^{2m}* CRE would be less methylated than the *VIP^{2}* CRE in DNA from hypothalamic tissue samples. Such differences in methylation could be a result of epigenetic variation alone, such that the same CpGs are methylated to different degrees on *VIP^{2}* and *VIP^{2m}*. Alternatively, because fixed differences in the *VIP* CRE create/disrupt CpGs, differential methylation could also be driven by genetic variation (Figure 2). Thus, I was interested in the extent to which methylation at shared vs. polymorphic sites contributes to overall differences in methylation. Second, does methylation of this CRE predict the expression of *VIP* in the same hypothalamic

tissue sample? I hypothesized that the degree of allele-specific methylation of the *VIP* CRE would predict the degree of expression of the corresponding allele in the same tissue samples. This study provides a first look at the extent to which differential epigenetic regulation of the ZAL2 and ZAL2^{m} alleles explains morph differences in *VIP* expression in the hypothalamus, and ultimately, morph differences in aggression in this species.

Methods

Tissues and Extractions

All procedures involving animals were approved by the Emory University Institutional Animal Care and Use Committee (IACUC), adhered to guidelines set forth by the National Institutes of Health Guide for the Care and Use of Laboratory Animals, and abided by all federal, state, and local laws. White-throated sparrows of both sexes and morphs were collected in the Hemlock Stream Forest in Argyle, Maine. Adults were collected early during the breeding season when territorial aggression was at its peak (Horton et al., 2014a; Horton et al., 2014b). We used song playback to lure adults into mist nets. There was no effect of morph or sex on latency to capture (Horton et al., 2014a; Horton et al., 2014b). We collected nestlings on post-hatch day seven, approximately two days before the natural fledging age in this species (Falls & Kopachena, 2020). Adults and nestlings were anesthetized with isoflurane and then euthanized by rapid decapitation. Brains were flash-frozen on powdered dry ice in the field and then shipped on dry ice to Emory University, where they were stored at -80°C until sectioning.

Microdissection of the hypothalamus was performed using previously established protocols (see Grogan et al., 2019; Merritt et al., 2020; Zinzow-Kramer et al., 2015). Briefly, adult and nestling brains were sectioned on a cryostat at 300 µm. Four hypothalamic punches from each brain were taken using a 1.0 mm punch tool (Palkovits, 1985). Punches were centered

on the midline to include both hemispheres of the hypothalamus. Two punches were taken in two consecutive sections. Within each section, the first of these punches was located immediately ventral to the anterior commissure. This punch included the caudal portion of the medial preoptic area (POM), the paraventricular nucleus (PVN), and the AH (Figure 3). The second punch, immediately ventral to the first, included the ventromedial hypothalamus (VMH) (Figure 3). In the adult samples, all four punches from each animal were pooled for RNA/DNA extraction, described below. In nestlings, because of the much higher yield of nucleic acids extracted, the dorsalmost punches from the two consecutive sections were pooled, as were the two ventralmost sections, to create two separate pools for each nestling. In both age groups, each pool of DNA was bisulfite-converted and sequenced separately. Then the data were averaged as necessary for statistical analysis. For further details on how these tissue samples were collected and processed, see Grogan et al. (2019), Merritt et al. (2020), and Zinzow-Kramer et al. (2015).

DNA and RNA were extracted from the punches using a Qiagen Allprep DNA/RNA micro kit (Qiagen, Valencia, CA, USA) with modifications described by Zinzow-Kramer et al. (2015), which allows total RNA and genomic DNA extraction from the same samples. We used the RNA for the RNA sequencing (described in the next section) and the DNA for bisulfite-converted sequencing to measure methylation (see below).

RNA Sequencing

Samples from adult males: Zinzow-Kramer and colleagues (2015) conducted the mRNA sequencing for the adult males at the Emory Yerkes Nonhuman Primate Genomics Core (Atlanta, GA). RNA libraries were constructed according to the manufacturer's protocol using the Illumina TruSeq RNA Sample Preparation Kit v2 (Illumina Inc., San Diego, CA, USA) and

sequenced on an Illumina HiSeq 1000 in 100 bp paired end-read reactions. For more detail, see Zinzow-Kramer et al. (2015).

Samples from adult females and nestlings: RNA library preparation and sequencing for the nestlings and adult females was performed by the Duke Center for Genomic and Computational Biology Sequencing and Genomic Technologies Core in Durham, NC. Libraries were constructed using a Kapa Stranded mRNA-Seq Kit (Kapa Biosystems, Boston, MA, USA) following the manufacturer's instructions, then sequenced on an Illumina HiSeq 4000 in 150 paired-end reactions. For more detail, see Merritt et al. (2020).

Measurements of Methylation

Bisulfite Conversion and Polymerase Chain Reaction

Two hundred nanograms of genomic DNA, extracted from the hypothalamus punches described above, were bisulfite-converted and prepared for sequencing with a Zymo EZ DNA Methylation Lightning Kit. Four primer pairs were designed using the Zymo Bisulfite Primer Seeker software (Zymo, Irvine, CA, USA) and included adapter sequences. Polymerase chain reaction (PCR) product lengths were 305-423 base pairs (bp) and spanned 28 SNPs and 74 CpG sites within the 1282 bp region upstream of the *VIP* transcription start site (NW_005081596.1:2258182-2259462; Table 1; Figure 2). I have operationally defined the *VIP* CRE in this study as this 1.2kb region. Each 25 µl PCR included 0.5 µl JumpStart Taq DNA polymerase, 2.5 µl JumpStart buffer containing 40 mM $MgCl_2$, 5 nM of each primer, and eight ng of bisulfite-converted DNA. Cycling conditions were 95°C for 60 seconds, then 40 cycles of 95°C for 30 seconds, 55°C for 30 seconds, and 70°C for 60 seconds, followed by a single final extension phase at 70°C for 5 min. Ten µl of each PCR product was visualized on a 1% agarose

gel. Any PCRs that did not show a band were rerun, modifying the concentration of $MgCl_2$ until a band of the expected size was visible.

Targeted Bisulfite Sequencing

Five microliters of each PCR product from all four primer pairs were pooled for each sample of the hypothalamus, for a total of 20 µl per bird. Before sequencing, these samples were indexed with the 16S Metagenomic Sequencing Library kit (Illumina; San Diego, CA, USA). At the Emory Integrated Genomics Core, samples were run on the Agilent bioanalyzer to confirm indexing and DNA quality. The samples were then pooled into a single lane and sequenced on an Illumina MiSeq (PE300).

Library Preparation

We obtained an average of 305,000 reads per sample. I assessed read quality with FastQC (Andrews, 2010) and trimmed the adapter sequences using Cutadapt (Martin, 2011). An average of 7000 reads per sample were filtered out based on a Phred score cutoff of 30, leaving about 298,000 reads per sample for data analysis. I then aligned these reads to a bisulfite-converted genome with Bowtie2 (Langmead & Salzberg, 2012). I created the bisulfite-converted genome with Bismark_genome_preparation (Krueger & Andrews, 2011) from a TS ZAL2 scaffold (NCBI accession: NW_005018596.1). The scaffold was N-masked at all SNPs except those disrupting CpG sites; the polymorphic CpG sites within the sequenced region were manually added to the reference genome to extract methylation status from all possible CpG sites, following Merritt et al. (2020). Reads with methylation at three or more non-CpG cytosines indicate possible incomplete bisulfite conversion or overestimated non-CG methylation and were filtered out (mean 3.6% per sample). I then identified the ZAL2 from the $ZAL2^m$ reads using SNPsplit by assigning reads to one of the two alleles based on the SNPs that did not affect CpGs.

I extracted methylation counts using the bismark_methylation_extractor (Kreuger & Andrews, 2011) and then used bismark2bedGraph to convert the output to bedGraph format, which I used for data analysis in R (version 3.6.2).

Data Analysis

All statistics were conducted in RStudio (RStudio Team 2020, R version 3.6.2). I conducted all analyses in adults and nestlings separately due to observed differences in both methylation and expression between the age groups (Sun et al., 2021). Additionally, ANOVAs in nestlings included a random effect of "nest" to account for sibling relatedness. I used Benjamini-Hochberg adjustments of the alpha levels to correct for multiple comparisons throughout this analysis (Benjamini & Hochberg, 1995).

The percent methylation of multiple CpG sites in one individual was greater than three times the standard deviation from the mean. This individual was also missing reads from all of the ZAL2^{m} amplicons, despite being labeled as a WS bird. Thus, I excluded this bird from all of the analyses.

Differences in Methylation

Bisulfite treatment converts unmethylated cytosines to thymines. Therefore, I calculated percent methylation at each CpG as the number of cytosine reads divided by the total number of cytosine and thymine reads at that site (Merritt et al., 2020). This calculation estimates the percentage of methylated CpGs out of the total number of CpGs. At polymorphic CpG sites, in other words, sites that are present on only one allele due to genetic variation, the allele that does not have the CpG was assigned zero percent methylation. Percent methylation was then averaged across the CRE to obtain an overall measure of percent methylation for each allele (*VIP*^{2} or *VIP*^{2m}) for each bird. Because the ZAL2 allele could be differentially methylated in TS vs. WS

birds, I needed to define *three* alleles in my data set: *VIP*^{2} CRE in TS birds (herein TS-*VIP*^{2}), the *VIP*^{2} CREs in WS birds (WS-*VIP*^{2}), and the *VIP*^{2m} CRE in WS birds (WS-*VIP*^{2m}).

To test for an effect of allele on percent methylation, I used ANOVAs within each age group. These ANOVAs included a random effect of individual to control for repeated measures (methylation of WS-*VIP*^{2} and WS-*VIP*^{2m}) in WS birds. I calculated the eta-squared (η^2) effect size for each of these ANOVAs. To determine which alleles were differently methylated, I conducted post-hoc ANOVAs to compare methylation between TS-*VIP*^{2} TS and WS-*VIP*^{2} and between WS-*VIP*^{2} and WS-*VIP*^{2m}. To determine the extent to which polymorphic CpGs drive allelic differences in methylation of the *VIP* CRE, I ran these analyses in parallel, with the polymorphic CpGs included and excluded.

To identify differentially methylated CpG sites, I conducted ANOVAs at each CpG to test for an effect of allele, with the same three levels as above (TS-*VIP*^{2}, WS-*VIP*^{2}, WS-*VIP*^{2m}), on percent methylation. As above, I followed up significant effects of allele with post-hoc ANOVAs to test for a difference between TS-*VIP*^{2} and WS-*VIP*^{2} and between WS-*VIP*^{2} and WS-*VIP*^{2m}.

Regressions of Methylation on Expression

To test whether methylation of the *VIP* CRE predicts *VIP* expression, I ran individual linear regressions of $\log_2$ transformed *VIP* read counts on methylation of the *VIP* CRE (Merritt et al., 2020). Each of these regressions was performed separately for each allele (TS-*VIP*^{2}; WS-*VIP*^{2}; WS-*VIP*^{2m}), using allele-specific reads and percent methylation of that allele within each age group. To test whether methylation of any individual CpG sites predicts expression, I ran separate analyses for each CpG. These analyses consisted of linear regressions of the percent

methylation of each CpG on the expression of the corresponding allele for a total of three sets of regressions (one per allele) at every CpG site in each age group.

Results

Differences in Methylation

In adults, ANOVA showed a significant main effect of allele on average percent methylation across the VIP CRE (Table 2). Post-hoc ANOVAs revealed that WS-VIP^{2m} was less methylated than WS-VIP^{2} (Figure 4A; Table 3). There was no difference in average percent methylation between TS-VIP2 and WS-VIP2 (Figure 4A; Table 3). After excluding polymorphic CpGs from these analyses, the effect of allele on percent methylation was stronger (Table 2), and the difference in percent methylation between VIP^{2} and VIP^{2m} persisted. In nestlings, these results were similar. The effect of allele on percent methylation was significant in the nestlings only when polymorphic CpGs were excluded (Figure 4B, Table 2), and post-hoc ANOVA showed that VIP^{2m} was less methylated than VIP^{2} when the polymorphic CpGs were excluded (Table 3).

In adults, there was an effect of allele on the percent methylation of eight out of the 66 individual CpGs that were shared between VIP^{2} and VIP^{2m} (Figure 5; Table 4). The results of post-hoc ANOVAs indicated that WS-VIP^{2m} was less methylated than WS-VIP^{2} at four of these shared sites and more methylated than WS-VIP^{2} at one of them (Figure 7A, Table 5). The remaining three shared CpGs were not significantly differentially methylated between the WS alleles (Figure 7A; Table 5). There were no differences between the morphs in the methylation of shared CpGs on VIP^{2}. In nestlings, there was an effect of allele for four out of 66 individual shared CpGs (Figure 6, Table 6). Among these, two were more methylated on WS-VIP^{2} and two

were more methylated on WS-*VIP*^{2m} (Figure 7B, Table 7). None of these sites, however, were differentially methylated between the WS- and TS-*VIP*^{2}.

In adults, all five of the ZAL2^{m}-specific CpGs were significantly methylated when compared with the assumed zero percent methylation of the corresponding (non-CpG) site on the ZAL2 allele (Figure 7A, Table 5). In contrast, only one of the three ZAL2-specific CpG sites that showed an effect of allele was significantly more methylated on TS-*VIP*^{2} than on WS-*VIP*^{2} (2259007; Figure 5A; Table 5). In nestlings, all eight of the polymorphic CpGs were significantly methylated in WS nestlings when compared with the corresponding non-CpG site (Figure 5B, Table 7). No sites, either shared or polymorphic, differed in methylation between WS-*VIP*^{2} and TS-*VIP*^{2}.

Regressions of Methylation on Expression

The average percent methylation of each CRE did not predict the expression of the corresponding allele in RNA extracted from the same tissues (Figure 8; Table 8). In contrast, *VIP* expression was predicted by methylation of some of the individual CpGs. After corrections for multiple comparisons, the methylation of only one individual CpG, which was located on *VIP*^{2}, predicted expression of that allele in adults (Figure 9; Tables 9-11). In nestlings, expression of TS-*VIP*^{2} was predicted by methylation of three individual CpGs on that allele (Figure 10; Tables 12-14).

Discussion

In the white-throated sparrow, a behavioral polymorphism in aggression results from a chromosomal rearrangement present in roughly half of the individuals in each population. Birds of the WS morph, which have a copy of the rearrangement, are more aggressive than birds of the TS morph. One of the genes captured by this rearrangement is *VIP*, the expression of which in

the AH is known to be causal for aggression in songbirds (Goodson et al., 2012a). In white-throated sparrows, *VIP* expression is higher in the AH of WS birds than TS birds, and it predicts territorial singing (Horton et al., 2020). These findings suggest that a morph differences in the regulation of this gene could at least partly explain the evolution of the behavioral polymorphism in this species. A potential explanation for the morph difference in *VIP* expression is allelic imbalance, such that VIP^{2m}, or the allele specific to WS birds, is expressed more than VIP^{2}. In this study, I tested whether the two alleles of *VIP* are subject to differential epigenetic regulation. I found that in samples of the hypothalamus, a regulatory region of VIP^{2m} was less methylated, on average, than the corresponding region of VIP^{2} in WS birds, and that VIP^{2} was not differentially methylated between WS-VIP^{2} and TS-VIP^{2}. This result is congruent with the morph difference in *VIP* expression described by Horton et al. (2020).

One way that methylation is likely to affect the expression of a gene is through the disruption of transcription factor binding (Eden & Cedar, 1994). Transcription factor binding sites tend to be only about ten nucleotides long (Stewart et al., 2012). Thus, in most consensus sequences, each nucleotide is essential for specific transcription factor binding. Point mutations (Prud'homme et al., 2006) or methylation (Okhovat et al., 2017) at even a single nucleotide can alter the expression of a gene. Hypomethylation of VIP^{2m} would therefore be concordant with the overall higher expression of *VIP* in the AH of WS birds. In this study, shared CpGs that were differentially methylated between VIP^{2} and VIP^{2m} were typically less methylated on VIP^{2m}. This result suggests that there may be more interactions between methylation and transcription factor binding on VIP^{2}, which may result in allelic imbalance in the expression of this gene.

Methylation and gene expression both change across development and in response to experience (Rubenstein et al., 2016; Sinha et al., 2020; Szyf et al., 2008). Thus, methylation of

the *VIP* allele could be a consequence, rather than a cause, of aggressive behavior. In this study, I found that the results in adults and nestlings were mostly similar and VIP^{2} and VIP^{2m} were already differentially methylated by post-hatch day seven. Because the morph difference in methylation arises early in development, these results suggest that differential methylation is not driven by morph differences in behavior observed in adulthood. This finding provides further support for the hypothesis that differential epigenetic regulation of the VIP gene could be a molecular mechanism underlying the behavioral polymorphism in this species.

In both age groups, there were many more CpG sites that were differentially methylated between the alleles in WS birds (14 sites in adults, 12 in nestlings) than VIP^{2} sites that were differentially methylated between the morphs (1 in adults, 0 in nestlings). This finding suggests that the epigenetic differentiation detected in this study is taking place largely within the rearrangement, instead of in a particular morph. Furthermore, although genetic variation within the *VIP* CRE has resulted in unique opportunities for methylation on each allele, not all of the differentially methylated CpGs were polymorphic. In fact, on the *VIP* CRE, allelic differences in methylation were stronger when the analysis excluded polymorphic CpGs (Figure 4). In other words, the differential methylation of the two alleles was not solely attributable to genetic differentiation. Instead, the allele-specific epigenetic differentiation between VIP^{2} and VIP^{2m} is occurring independently of genetic differentiation.

In a similar study on another gene inside the rearrangement, *ESR1*, Merritt et al. (2020) found that the allelic differences in methylation of a CRE disappeared when excluding polymorphic sites (Merritt et al., 2020). In other words, there was no effect of allele on the methylation of the *ESR1* CRE if the polymorphic CpGs were excluded. This result suggests that the difference in methylation between the ZAL2 and $ZAL2^{m}$ alleles was driven by allele-specific

opportunities for methylation created by genetic differentiation between the alleles. In this study of *VIP*, the effect of allele on methylation was stronger after excluding the polymorphic CpGs (Figure 4). This finding suggests that the differential methylation between VIP^{2} and VIP^{2m} is not driven by genetic differentiation between the alleles, as was the case with ESR1, but rather that the differential methylation of the VIP alleles is driven by epigenetic factors.

The contrast between the mechanisms underlying differential methylation of the ESR1 and VIP CREs suggests that the degree of true epigenetic regulation within the $ZAL2/2^{m}$ rearrangement may vary by gene. An investigation of chromosome-wide methylation of $ZAL2/2^{m}$ revealed variation in the degree and direction of differences between the alleles, such that $ZAL2^{m}$ was sometimes hypermethylated, hypomethylated, or extremely hypomethylated depending on the location (Sun et al., 2021). Together, these results suggest that, instead of a general effect of the rearrangement on gene expression, there may be mutiple mechanisms, both genetic and epigenetic, that regulate the expression of the $ZAL2/2^{m}$ alleles.

The $ZAL2/2^{m}$ rearrangement has captured over 1000 genes, and it is very likely that the behavioral polymorphism in this species is affected by interactions among multiple co-adapted genes within the rearrangement (Dobzhansky, 1950; Maney et al., 2020; Sinha et al., 2020). Thus, regardless of the extent to which *VIP* is epigenetically regulated, I expect that there are morph-specific, trans-regulatory effects of other ZAL2/2m genes on the expression of this gene. For example, there are morph differences in sex steroids (Maney et al., 2009), which are known to affect gene expression and to play a role in phenotypic integration (Cox, 2020). The VIP gene is known to be regulated by sex steroids in other species (Gozes et al., 1989; Aste et al., 1997; Wacker et al., 2008), meaning that a morph difference in sex steroid levels could itself lead to a morph difference in VIP expression regardless of variation in the VIP CRE. Sex steroid receptors

can act as transcription factors, meaning that local variation in methylation or genetic sequence can affect their binding, creating further allelic differences in opportunities for cis-regulation. Moreover, enhancer elements can affect gene expression from millions of base pairs away (Pennacchio et al., 2013) so other, co-adapted alleles within the ZAL2/2^{m} rearrangement may also contribute to morph differences in VIP expression and, consequently, behavioral polymorphism in aggression (Maney et al., 2020).

In this study, I hypothesized that if the morph difference in VIP expression is caused by differential methylation of the VIP^{2m} and VIP^{2} alleles, then methylation of either allele should predict the expression of that allele. Despite finding evidence of allelic differences in methylation, I found that the overall average methylation of a particular *VIP* allele did not predict expression of that allele in this data set. In contrast, methylation of several individual CpGs significantly predicted expression. Such associations might indicate the location of a binding site for a transcription factor that interacts with a particular allele or at a particular developmental stage. Although some of those correlations seemed to be driven by a single individual (Figures 9-10), it may be worth investigating possible transcription factor binding at these locations.

The lack of a relationship between methylation and expression in this study could be explained by a number of factors. First, the sequenced regulatory region was located directly upstream of the transcription start site. Across taxa, the region nearest to the transcription start site of any given gene tends to be hypomethylated (Suzuki & Bird, 2008). The hypomethylation of this narrow sequencing window could explain the relatively low averages and variation in percent methylation in this data set in contrast with chromosome-wide methylation (Sun et al., 2021) and the methylation of a nearby gene (Merritt et al., 2020). The relatively limited variation

in methylation of this region may have reduced the chances of detecting a relationship between methylation and expression.

Second, the region sequenced in this study was relatively short, only 1.2kb. Many other genetic sequences associated with the *VIP* gene could affect *VIP* expression, but those were not included in this study. For instance, CREs can affect gene transcription from up to 10kb upstream (Suzuki & Bird, 2008). In the case of *VIP*, the upstream sequence is limited because the next gene upstream, *MYCT1*, is about 5kb away; thus it may be feasible to capture nearly all of the upstream regulatory variation by sequencing a relatively short DNA segment.. There are also potential effects of methylation of regions that are not directly upstream of the transcription start sites. For example, CREs can affect gene expression from within introns (Suzuki & Bird, 2008). Sequencing bisulfite-converted DNA over this entire region, including the introns and other untranslated regions, would permit a clearer picture of the methylation landscape of the *VIP* CRE and the potential effect of methylation on expression.

A third potential reason that methylation did not predict expression in this study is related to the tissue sampling itself. The tissue punches used in this study included several nuclei within the mediobasal hypothalamus in addition to the AH, including the PVN, VMH, and caudal POM. All of these brain regions contain VIP cell populations that could be unrelated to aggression (reviewed by Kingsbury & Wilson, 2016). Another region of the mediobasal hypothalamus, located just ventral to the VMH, is the infundibular nucleus (INF). *VIP* in the INF acts as a releasing factor for prolactin, which is strongly associated with parenting in birds (Macnamee et al., 1986; Maney et al., 1999; reviewed by Smiley, 2019). Parental care is part of the behavioral phenotype associated with the ZAL2^{m} rearrangement; TS birds exhibit more parental behavior than WS birds of the same sex (Horton et al., 2014b; Knapton & Falls, 1983; Kopachena & Falls,

1993). In a previous study, we found that *VIP* expression in the INF is higher in TS males than in WS males (Horton et al., 2020), which is opposite in direction to the morph difference in the AH. Thus, I would predict that the pattern of *VIP* methylation in INF is also opposite to that in the AH. That is, the VIP^{2m} allele should be more methylated than the VIP^{2} allele in INF. Although we intended to avoid sampling INF in this study (Figure 2), depending on the plane of section, INF may have been partially captured in some of the samples. This heterogeneity of the VIP populations in the samples could have interfered with the detection of the relationships between methylation and expression that may be unique to AH cell populations. In future studies, precise punches of individual hypothalamic nuclei will help reveal interactions between region-specific expression and methylation of *VIP*.

Altogether, these results provide evidence of allelic differences in the methylation of the *VIP* CRE in the hypothalamus of white-throated sparrows. It is yet unclear whether these differences contribute to allelic imbalance of *VIP*, and subsequently morph differences in aggression. This study serves as an important first look at the potential role of methylation in the expression of *VIP*, as we continue to learn about the complex genetics underlying the behavioral polymorphism in this species. The white-throated sparrow model continues to provide rich opportunities to explore the complex gene regulatory networks that drive behavioral phenotypes, ultimately shedding light on the molecular mechanisms underlying behavioral evolution.

References

Andrews S. (2010). FastQC: a quality control tool for high throughput sequence data. Available online at: http://www.bioinformatics.babraham.ac.uk/projects/fastqc

Aste, N., Viglietti-Panzica, C., Balthazart, J., & Panzica, G. (1997). Testosterone modulation of peptidergic pathways in the septo-preoptic region of male Japanese quail. *Avian and Poultry Biology Reviews, 8,* 77–93.

Benjamini, Y., & Hochberg, Y. (1995). Controlling the false discovery rate: A practical and powerful approach to multiple testing. *Journal of the Royal Statistical Society, 57*(1), 289–300.

Bullock, T. H. (1984). Comparative neuroscience holds promise for quiet revolutions. *Science*, *225*(4661), 473–478.

Campagna, L. (2016). Supergenes: The genomic architecture of a bird with four sexes. *Current Biology*, *26*(3), R105–R107.

Cox, R. M. (2020). Sex steroids as mediators of phenotypic integration, genetic correlations, and evolutionary transitions. *Molecular and Cellular Endocrinology, 502,* 110668.

Davis, J. K., Mittel, L. B., Lowman, J. J., Thomas, P. J., Maney, D. L., Martin, C. L., & Thomas, J. W. (2011). Haplotype-based genomic sequencing of a chromosomal polymorphism in the white-throated sparrow (*Zonotrichia albicollis*). *Journal of Heredity*, *102*(4), 380–390.

Dobzhansky, T., 1950. Genetics of natural populations. XIX. Origin of heterosis through natural selection in populations of *Drosophila pseudoobscura*. *Genetics 35 (3),* 288.

Eden, S. & Cedar, H. (1994). Role of DNA methylation in the regulation of transcription. *Current Opinion in Genetics & Development*, *4*(2), 255–259.

Falls, J. B. and J. G. Kopachena (2020). White-throated Sparrow (*Zonotrichia albicollis*), version 1.0. In *Birds of the World* (A. F. Poole, Editor). Cornell Lab of Ornithology, Ithaca, NY, USA.

Goodson, J. L. (1998). Territorial aggression and dawn song are modulated by septal vasotocin and vasoactive intestinal polypeptide in male field sparrows (*Spizella pusilla*). *Hormones and Behavior*, *34*(1), 67–77.

Goodson, J. L., Kelly, A. M., Kingsbury, M. A., & Thompson, R. R. (2012a). An aggression-specific cell type in the anterior hypothalamus of finches. *Proceedings of the National Academy of Sciences U.S.A., 109*(34), 13847–13852.

Goodson, J. L., Wilson, L. C., & Schrock, S. E. (2012b). To flock or fight: Neurochemical signatures of divergent life histories in sparrows. *Proceedings of the National Academy of Sciences U.S.A., 109*, 10685–10692.

Gozes, I., Werner, H., Fawzi, M., Abdelatty, A., Shani, Y., Fridkin, M., & Koch, Y. (1989). Estrogen regulation of vasoactive intestinal peptide mRNA in rat hypothalamus. *Journal of Molecular Neuroscience,* 1(1), 55–61.

Grogan, K. E., Horton, B. M., Hu, Y., & Maney, D. L. (2019). A chromosomal inversion predicts the expression of sex steroid-related genes in a species with alternative behavioral phenotypes. *Molecular and Cellular Endocrinology*, *495*, 110517.

Heberle, E., & Bardet, A. F. (2019). Sensitivity of transcription factors to DNA methylation. *Essays in Biochemistry*, *63*(6), 727–741.

Horton, B. M., Hauber, M. E., & Maney, D. L. (2012). Morph matters: Aggression bias in a polymorphic sparrow. *PLoS ONE, 7*(10), e48705.

Horton, B. M., Hu, Y., Martin, C. L., Bunke, B. P., Matthews, B. S., Moore, I. T., Thomas, J. W., & Maney, D. L. (2013). Behavioral characterization of a white-throated sparrow homozygous for the ZAL2^{m} chromosomal rearrangement. *Behavior Genetics*, *43*(1), 60–70.

Horton, B. M., Hudson, W. H., Ortlund, E. A., Shirk, S., Thomas, J. W., Young, E. R., Zinzow-Kramer, W. M., & Maney, D. L. (2014a). Estrogen receptor α polymorphism in a species with alternative behavioral phenotypes. *Proceedings of the National Academy of Sciences U.S.A.*, *111*(4), 1443–1448.

Horton, B. M., Michael, C. M., Prichard, M. R., & Maney, D. L. (2020). Vasoactive intestinal peptide as a mediator of the effects of a supergene on social behaviour. *Proceedings of the Royal Society B: Biological Sciences*, *287*(1924), 20200196.

Horton, B. M., Moore, I. T., & Maney, D. L. (2014b). New insights into the hormonal and behavioural correlates of polymorphism in white-throated sparrows, *Zonotrichia albicollis*. *Animal Behavior*, *93*, 207–219.

Huynh, L. Y., Maney, D. L., & Thomas, J. W.. (2011). Chromosome-wide linkage disequilibrium caused by an inversion polymorphism in the white-throated sparrow (*Zonotrichia albicollis*). *Heredity*, *106*(4), 537.

Joron, M., & Whibley, A. (2011). Stripes, sex and sparrows: What processes underlie heteromorphic chromosome evolution? *Heredity*, *106*(4), 531–532.

Keifer, J., & Summers, C. H. (2016). Putting the “Biology” back into “Neurobiology”: The strength of diversity in animal model systems for neuroscience research. *Frontiers in Systems Neuroscience*, *10*, 69.

Kingsbury, M. A. (2015). New perspectives on vasoactive intestinal polypeptide as a widespread modulator of social behavior. *Current Opinion in Behavioral Sciences*, *6*, 139–147.

Kingsbury, M. A., & Wilson, L. C. (2016). The role of VIP in social behavior: Neural hotspots for the modulation of affiliation, aggression, and parental care. *Journal of Integrative and Comparative Biology*, *56*(6), 1238–1249.

Knapton, R. W., & Falls, J. B. (1983). Differences in parental contribution among pair types in the polymorphic white-throated sparrow. *Canadian Journal of Zoology*, *61*(6), 1288–1292.

Kopachena, J. G., & Falls, J. B. (1993a). Aggressive performance as a behavioral correlate of plumage polymorphism in the white-throated sparrow (*Zonotrichia albicollis*). *Behaviour*, *124*(3/4), 249–266.

Kopachena, J. G., & Falls, J. B. (1993b). Re-evaluation of morph-specific variations in parental behavior of the white-throated sparrow. *The Wilson Bulletin*, 48–59.

Krueger, F., & Andrews, S. R. (2011). Bismark: A flexible aligner and methylation caller for Bisulfite-Seq applications. *Bioinformatics*, *27*(11), 1571–1572.

Krueger, Felix, & Andrews, S. R. (2016). SNPsplit: Allele-specific splitting of alignments between genomes with known SNP genotypes. *F1000Research*, *5*, 1479–1479.

Kuenzel, W. J., McCune, S. K., Talbot, R. T., Sharp, P. J., & Hill, J. M. (1997). Sites of gene expression for vasoactive intestinal polypeptide throughout the brain of the chick (*Gallus domesticus*). *Journal of Comparative Neurology*, *381*(1), 101–118.

Langmead, B., & Salzberg, S. L. (2012). Fast gapped-read alignment with Bowtie 2. *Nature Methods*, *9*(4), 357–359.

Lowther, J. K. (1961). Polymorphism in the white-throated sparrow, *Zonotrichia albicollis* (Gmelin). *Canadian Journal of Zoology*, *39*(3), 281–292.

Macnamee, M. C., Sharp, P. J., Lea, R. W., Sterling, R. J., & Harvey, S. (1986). Evidence that vasoactive intestinal polypeptide is a physiological prolactin-releasing factor in the bantam hen. *General and Comparative Endocrinology*, *62*(3), 470–478.

Mamrut, S., Harony, H., Sood, R., Shahar-Gold, H., Gainer, H., Shi, Y. J., Barki-Harrington, L., & Wagner, S. (2013). DNA methylation of specific CpG sites in the promoter region regulates the transcription of the mouse oxytocin receptor. *PLoS ONE*, *8*(2), e56869.

Maney, D. L. (2008). Endocrine and genomic architecture of life history trade-offs in an avian model of social behavior. *General and Comparative Endocrinology*, *157*(3), 275–282.

Maney, D. L., Horton, B. M., & Zinzow-Kramer, W. M. (2015). Estrogen receptor alpha as a mediator of life-history trade-offs. *Integrative and Comparative Biology*, *55*(2), 323–331.

Maney, D. L., Lange, H. S., Raees, M. Q., Reid, A. E., & Sanford, S. E. (2009). Behavioral phenotypes persist after gonadal steroid manipulation in white-throated sparrows. *Hormones and Behavior*, *55*(1), 113–120.

Maney, D. L., Merritt, J. R., Prichard, M. R., Horton, B. M., & Yi, S. V. (2020). Inside the supergene of the bird with four sexes. *Hormones and Behavior*, *126*, 104850.

Maney, D. L., Schoech, S. J., Sharp, P. J., & Wingfield, J. C. (1999). Effects of vasoactive intestinal peptide on plasma prolactin in passerines. *Journal of General and Comparative Endocrinology*, *113*(3), 323–330.

Manger, P. R., Cort, J., Ebrahim, N., Goodman, A., Henning, J., Karolia, M., Rodrigues, S. L., & Strkalj, G. (2008). Is 21st century neuroscience too focussed on the rat/mouse model of brain function and dysfunction? *Frontiers in Neuroanatomy*, *2*, 5.

Martin, M. (2011). Cutadapt removes adapter sequences from high-throughput sequencing reads. *EMBnet.Journal*, *17*(1), 10–12.

Mendizabal, I., & Yi, S. V. (2016). Whole-genome bisulfite sequencing maps from multiple human tissues reveal novel CpG islands associated with tissue-specific regulation. *Human Molecular Genetics*, *25*(1), 69–82.

Merritt, J. R., Grogan, K. E., Zinzow-Kramer, W. M., Sun, D., Ortlund, E. A., Yi, S. V., & Maney, D. L. (2020). A supergene-linked estrogen receptor drives alternative phenotypes in a polymorphic songbird. *Proceedings of the National Academy of Sciences U.S.A.*, 202011347.

Montagnese, C. M., Székely, T., Csillag, A., & Zachar, G. (2015). Distribution of vasotocin- and vasoactive intestinal peptide-like immunoreactivity in the brain of blue tit (*Cyanistes coeruleus*). *Frontiers in Neuroanatomy*, *9*, 90–90.

Okhovat, M., Maguire, S. M., & Phelps, S. M. (2017). Methylation of avpr1a in the cortex of wild prairie voles: Effects of CpG position and polymorphism. *Royal Society Open Science*, *4*(1), 160646.

Palkovits, M. (1985). Microdissection of individual brain nuclei and areas. In *General Neurochemical Techniques* (pp. 1-17). Humana Press, Totowa, NJ.

Pennacchio, L. A., Bickmore, W., Dean, A., Nobrega, M. A., & Bejerano, G. (2013). Enhancers: Five essential questions. *Nature Reviews Genetics*, *14*(4), 288–295.

Prud'homme, B., Gompel, N., Rokas, A., Kassner, V. A., Williams, T. M., Yeh, S.-D., True, J. R., & Carroll, S. B. (2006). Repeated morphological evolution through cis -regulatory changes in a pleiotropic gene. *Nature*, *440*(7087), 1050–1053.

Rubenstein, D. R., Skolnik, H., Berrio, A., Champagne, F. A., Phelps, S., & Solomon, J. (2016). Sex-specific fitness effects of unpredictable early life conditions are associated with DNA methylation in the avian glucocorticoid receptor. *Molecular Ecology*, *25*(8), 1714–1728.

Sinha, S., Jones, B. M., Traniello, I. M., Bukhari, S. A., Halfon, M. S., Hofmann, H. A., Huang, S., Katz, P. S., Keagy, J., Lynch, V. J., Sokolowski, M. B., Stubbs, L. J., Tabe-Bordbar, S., Wolfner, M. F., & Robinson, G. E. (2020). Behavior-related gene regulatory networks: A new level of organization in the brain. Proc Natl Acad Sci U S A. https://doi.org/10.1073/pnas.1921625117

Smiley, K. O. (2019). Prolactin and avian parental care: New insights and unanswered questions. *Hormones and Behavior*, *11*, 114–130.

Stewart, A. J., Hannenhalli, S., & Plotkin, J. B. (2012). Why transcription factor binding sites are ten nucleotides long. *Genetics*, *192*(3), 973–985.

Sun, D., Huh, I., Zinzow-Kramer, W. M., Maney, D. L., & Yi, S. V. (2018). Rapid regulatory evolution of a nonrecombining autosome linked to divergent behavioral phenotypes. *Proceedings of the National Academy of Sciences*, *115*(11), 2794–2799.

Sun, D., Layman, T. S., Jeong, H., Chatterjee, P., Grogan, K., Merritt, J. R., ... & Yi, S. V. (2021). Genome-wide variation in DNA methylation linked to developmental stage and chromosomal suppression of recombination in white-throated sparrows. *Molecular Ecology*.

Suzuki, M. M., & Bird, A. (2008). DNA methylation landscapes: Provocative insights from epigenomics. *Nature Reviews Genetics*, *9*(6), 465–476.

Szyf, M., McGowan, P., & Meaney, M. J. (2008). The social environment and the epigenome. *Environmental and Molecular Mutagenesis, 49*(1), 46–60.

Thompson, R. R. (2020). An updated field guide for snark hunting: Comparative contributions to behavioral neuroendocrinology in the era of model organisms. *Hormones and Behavior, 122*, 104742.

Thorneycroft, H. B. (1975). A cytogenetic study of the white-throated sparrow, *Zonotrichia albicollis* (Gmelin). *Journal of Evolution, 29*(4), 611–621.

Tuttle, E. M. (2003). Alternative reproductive strategies in the white-throated sparrow: Behavioral and genetic evidence. *Behavioral Ecology*, *14*(3), 425–432.

Tuttle, E. M., Bergland, A. O., Korody, M. L., Brewer, M. S., Newhouse, D. J., Minx, P., Stager, M., Betuel, A., Cheviron, Z. A., Warren, W. C., Gonser, R. A., & Balakrishnan, C. N. (2016). Divergence and functional degradation of a sex chromosome-like supergene. *Current Biology, 26*(3), 344–350.

Wacker, D. W., Schlinger, B. A., & Wingfield, J. C. (2008). Combined effects of DHEA and fadrozole on aggression and neural VIP immunoreactivity in the non-breeding male song sparrow. *Hormones and Behavior, 53*(1), 287–294.

Zinzow-Kramer, W. M., Horton, B. M., McKee, C. D., Michaud, J. M., Tharp, G. K., Thomas, J. W., Tuttle, E. M., Yi, S., & Maney, D. L. (2015). Genes located in a chromosomal inversion are correlated with territorial song in white-throated sparrows. *Genes, Brain, and Behavior*, *14*(8), 641–654.

Tables

Table 1

PCR primer sets used to amplify portions of the cis-regulatory region of VIP *in bisulfite-converted DNA.*

Amplicon	F (5'-3') R (5'-3')	Start	End
1	**F:** AGTAATAAGGGGAAAATTTTTTGAAATTAGATTATTG **R:** TTTTTCTTAAATTTTTATACCTCTAATCCTCCTAC	2258182	2258487
2	**F:** AGAATTTTYGGTATTGAGTTTGTTTAATTTTTAGTG **R:** TCCTTCRAATTTTACCTACCTCAAAAAAAT	2258333	2258713
3	**F:** TTTTTTTTTYGTTGTTTAGATTTTTTTGAGG **R:** ATCCCCRACACATACAAATCCCTAATAAAAATTCCTAC	2258666	2259089
4	**F:** GTATTTYGGGTAGGAATTTTTATTAGGGATTTGTATG **R:** AAAACAATCAAAAACTTATATTTAACACATAAACAAC	2259043	2259462

Note. Sequences are given for each primer pair used for amplicons 1 – 4 (Figure 2), along with start and end positions on the ZAL2 genomic scaffold (NCBI: NW_005081596.1). Nextera sequences were appended to the beginning of both forward and reverse primers before amplification. Forward Nextera sequence: TCGTCGGCAGCGTCAGATGTGTATAAGAGACAG. Reverse Nextera sequence: GTCTCGTGGGCTCGGAGATGTGTATAAGAGACAG.

Table 2

Results of ANOVAs testing the effect of allele on percent methylation of the VIP *CRE.*

Age Group	Poly CpGs	P-value	df	F-statistic	Eta^2
adult	included	0.014 ∗	2,10	6.824	0.577
	excluded	0.004 ∗	2,10	10.140	0.670
nestling	included	0.316	2,9	1.315	0.226
	excluded	0.047 ∗	2,9	4.388	0.494

Note. Results are presented for models that included or excluded polymorphic ("Poly") CpGs.

∗ $p < 0.05$

Table 3

Post-hoc t-tests for effects of allele on percent methylation of the VIP *CRE in adults and nestlings.*

			Included [1]		Excluded [2]	
Age Group	Alleles	Test	t-value	P-value	t-value	P-value
adult	ZAL2-WS, ZAL2-TS	unpaired	-0.687	0.500	-0.763	0.454
adult	ZAL2-WS, ZAL2m-WS	paired	3.323	0.004 ∗	4.414	0.001 ∗
nestling	ZAL2-WS, ZAL2-TS	unpaired	-1.423	0.177	-1.429	0.178
nestling	ZAL2-WS, ZAL2m-WS	paired	1.258	0.237	2.767	0.019 ∗

∗ $p < 0.05$

1 All CpGs on each allele included, including polymorphic CpGs.

[2] Polymorphic CpGs are excluded, leaving the data set with only shared CpGs.

Table 4

Results of ANOVAs testing for effects of allele on percent methylation of each CpG in the VIP *CRE in adults.*

CpG position	F-statistic	P-value		df	Eta^2
2258251	0.7953	0.3794		1	0.025
2258330	0.3004	0.5875		1	0.01
2258341	1.1587	0.2898		1	0.035
2258417	50.7084	0.0000	∗	1	0.613
2258431	30.9632	0.0000	∗	1	0.534
2258440	4.8579	0.0348	∗	1	0.132
2258539	0.1414	0.7094		1	0.004
2258541	1.2103	0.2795		1	0.036
2258572	0.5245	0.4742		1	0.016
2258582	2.3478	0.1356		1	0.07
2258616	12.0691	0.0025	∗	1	0.388
2258619	0.3079	0.5831		1	0.01
2258627	0.4113	0.5263		1	0.014
2258632	4.0363	0.0543		1	0.126
2258636	1.2489	0.2753		1	0.052
2258638	3.5404	0.0721		1	0.129
2258647	2.2807	0.1440		1	0.087
2258674	4.9438	0.0339	∗	1	0.141
2258707	0.6873	0.4125		1	0.019
2258760	0.9259	0.3423		1	0.025
2258795	19.9405	0.0001	∗	1	0.356
2258806	0.1771	0.6764		1	0.005
2258830	5.3208	0.0269	∗	1	0.129
2258839	2.1198	0.1541		1	0.056
2258841	0.0009	0.9768		1	0
2258850	1.5548	0.2205		1	0.041
2258852	1.3941	0.2455		1	0.037
2258858	0.0292	0.8654		1	0.001
2258863	4.6486	0.0378	∗	1	0.114
2258869	0.0897	0.7663		1	0.002
2258880	0.9635	0.3329		1	0.026
2258884	0.1216	0.7294		1	0.003
2258890	2.7988	0.1030		1	0.072
2258893	3.0054	0.0915		1	0.077
2258906	2.2727	0.1404		1	0.059
2258910	0.9175	0.3445		1	0.025
2258928	0.7493	0.3924		1	0.02
2258937	6.3506	0.0163	∗	1	0.15

2258943	0.0826	0.7755		1	0.002
2258947	1.6642	0.2053		1	0.044
2259007	5.7732	0.0216	∗	1	0.138
2259042	1.1686	0.2869		1	0.031
2259049	8.4436	0.0062	∗	1	0.19
2259083	5.3554	0.0265	∗	1	0.129
2259110	1.1922	0.2849		1	0.044
2259122	1.7728	0.1946		1	0.064
2259150	1.3063	0.2635		1	0.048
2259153	0.5592	0.4613		1	0.021
2259155	0.5901	0.4493		1	0.022
2259179	3.7441	0.0639		1	0.126
2259207	2.3546	0.1375		1	0.086
2259224	2.2289	0.1503		1	0.096
2259236	0.0652	0.8007		1	0.003
2259241	0.1828	0.6728		1	0.008
2259250	3.0880	0.0916		1	0.114
2259256	4.3681	0.0469	∗	1	0.149
2259268	0.0205	0.8872		1	0.001
2259270	0.4804	0.4946		1	0.019
2259278	2.5391	0.1236		1	0.092
2259280	0.0174	0.8960		1	0.001
2259284	0.2102	0.6506		1	0.008
2259293	0.3034	0.5871		1	0.013
2259296	1.3954	0.2496		1	0.057
2259300	0.0611	0.8070		1	0.003
2259303	1.0233	0.3223		1	0.043
2259312	3.5506	0.0722		1	0.134
2259319	12.6248	0.0017	∗	1	0.354
2259324	2.2366	0.1484		1	0.089
2259338	0.3131	0.5817		1	0.015
2259341	0.2677	0.6103		1	0.013
2259349	0.3709	0.5488		1	0.017
2259392	1.2380	0.2784		1	0.056
2259422	0.8904	0.3552		1	0.037
2259424	0.1223	0.7297		1	0.005

∗ indicates a statistically significant effect of allele after Benjamini-Hochberg correction.

Table 5

Results of post-hoc ANOVAs testing for effects of allele on percent methylation for each CpG in adults.

	WS ZAL2 / WS ZAL2m				WS ZAL2 / TS ZAL2			
Position	F-statistic	P-value	df		F-statistic	P-value	df	
2258417	22.3804	0.0021	1,7	∗		N/A[1]		
2258431	15.5869	0.0055	1,7	∗		N/A[1]		
2258440	5.6259	0.0495	1,7	∗	2.8488	0.1044	1	
2258616	7.1831	0.0315	1,7	∗		N/A[1]		
2258674	12.2341	0.0100	1,7	∗	0.0689	0.7954	1	
2258795	8.9054	0.0124	1, 11	∗		N/A[1]		
2258830	4.5955	0.0552	1, 11		0.1219	0.7300	1	
2258863	5.0417	0.0463	1, 11	∗	0.0088	0.9259	1	
2258937	2.7043	0.1283	1, 11		0.4430	0.5120	1	
2259007	6.2817	0.0292	1, 11	∗	7.1539	0.0133	1	∗
2259049	23.7921	0.0005	1, 11	∗	3.0329	0.0944	1	
2259083	16.6534	0.0018	1, 11	∗	2.9011	0.1014	1	
2259256	3.0152	0.1261	1,7		0.8807	0.3611	1	
2259319	5.6506	0.0491	1, 11	∗		N/A[1]		

Note. CpGs are listed in order relative to their location in the sequence. ANOVAs in WS birds included a random effect of individual to account for within-subjects measurement of each allele.

∗ Indicates statistical significance after Benjamini-Hochberg correction.

[1] ZAL2^{m}-specific CpGs

Table 6

Results of ANOVAs testing for effects of allele on percent methylation for each CpG in nestlings.

Position	F-statistic	P-value		df [a]	Eta^2
2258251	0.0107	0.9202		1,8	0.001
2258330	2.0485	0.1902		1,8	0.204
2258341	28.5367	0.0003	∗	1,10	0.741
2258417	21.9632	0.0009	∗	1,10	0.687
2258431	37.5768	0.0001	∗	1,10	0.79
2258440	12.9969	0.0048	∗	1,10	0.565
2258539	0.5298	0.4834		1,10	0.05
2258541	3.4697	0.0921		1,10	0.258
2258572	2.4513	0.1485		1,10	0.197
2258582	9.3641	0.0120	∗	1,10	0.484
2258616	5.5982	0.0395	∗	1,10	0.359
2258619	0.5878	0.4610		1,10	0.056
2258627	3.1322	0.1072		1,10	0.239
2258632	0.0981	0.7606		1,10	0.01
2258636	0.0179	0.8962		1,10	0.002
2258638	3.4793	0.0917		1,10	0.258
2258647	2.7953	0.1255		1,10	0.218
2258674	1.1465	0.3094		1,10	0.103
2258707	0.0680	0.7994		1,10	0.007
2258760	0.1370	0.7190		1,10	0.014
2258795	26.5190	0.0004	∗	1,10	0.726
2258806	0.0345	0.8564		1,10	0.003
2258830	0.2232	0.6468		1,10	0.022
2258839	2.0840	0.1794		1,10	0.172
2258841	0.4407	0.5218		1,10	0.042
2258850	1.5101	0.2473		1,10	0.131
2258852	0.2457	0.6308		1,10	0.024
2258858	0.0944	0.7650		1,10	0.009
2258863	3.6552	0.0849		1,10	0.268
2258869	1.6995	0.2216		1,10	0.145
2258880	1.5296	0.2444		1,10	0.133
2258884	1.2116	0.2968		1,10	0.108
2258890	1.7253	0.2184		1,10	0.147
2258893	0.3543	0.5649		1,10	0.034
2258906	2.8773	0.1207		1,10	0.223
2258910	1.8067	0.2086		1,10	0.153
2258928	2.6957	0.1317		1,10	0.212
2258937	0.1017	0.7563		1,10	0.01
2258943	1.0726	0.3248		1,10	0.097
2258947	1.8583	0.2027		1,10	0.157

2259007	8.8154	0.0141	∗	1,10	0.469
2259042	0.7881	0.3955		1,10	0.073
2259049	16.3139	0.0024	∗	1,10	0.62
2259083	23.9225	0.0006	∗	1,10	0.705
2259110	1.0341	0.3358		1, 9	0.103
2259122	1.3937	0.2680		1, 9	0.134
2259150	0.4094	0.5382		1, 9	0.044
2259153	0.4802	0.5058		1, 9	0.051
2259155	5.1052	0.0502		1, 9	0.362
2259179	0.8398	0.3834		1, 9	0.085
2259207	0.5617	0.4727		1, 9	0.059
2259224	12.6784	0.0162	∗	1,5	0.717
2259236	3.6785	0.0873		1, 9	0.29
2259241	1.2412	0.2941		1, 9	0.121
2259250	0.2237	0.6475		1, 9	0.024
2259256	0.8221	0.3882		1, 9	0.084
2259268	3.9182	0.0791		1, 9	0.303
2259270	2.8699	0.1245		1, 9	0.242
2259278	1.5581	0.2434		1, 9	0.148
2259280	0.4819	0.5051		1, 9	0.051
2259284	0.3999	0.5429		1, 9	0.043
2259293	0.3060	0.5936		1, 9	0.033
2259296	0.3788	0.5535		1, 9	0.04
2259300	0.5552	0.4752		1, 9	0.058
2259303	1.4608	0.2576		1, 9	0.14
2259312	0.9022	0.3670		1, 9	0.091
2259319	20.6237	0.0014	∗	1, 9	0.696
2259324	3.5676	0.0915		1, 9	0.284
2259338	0.8111	0.3912		1, 9	0.083
2259341	4.8240	0.0557		1, 9	0.349
2259349	2.1538	0.1804		1, 9	0.212
2259392	1.0379	0.3381		1, 9	0.115
2259422	1.9397	0.1971		1, 9	0.177
2259424	1.2623	0.2903		1, 9	0.123

Note. CpGs are listed in order relative to their location in the sequence.

∗ Indicates statistical significance after Benjamini-Hochberg correction.

[a] Variability in the degrees of freedom was caused by variation in the availability of full-length reads for each bird and thus variation in the coverage at each CpG site, resulting in some missing data at individual CpGs for some birds.

Table 7

Results of post-hoc ANOVAs testing for effects of allele on percent methylation of each CpG in nestlings.

	WS ZAL2 / WS ZAL2m				WS ZAL2 / TS ZAL2		
position	F-statistic	p-value	df		F-statistic	p-value	df
2258341	28.4921	0.0003	1, 10	∗	0.2598	0.6195	1, 12
2258417	12.3853	0.0055	1, 10	∗		-	
2258431	15.7997	0.0073	1, 6	∗		-	
2258440	12.8432	0.0050	1, 10	∗	0.5533	0.4713	1, 12
2258582	9.9732	0.0102	1, 10	∗	2.0482	0.1779	1, 12
2258616	3.1569	0.1060	1, 10			-	
2258795	14.9545	0.0031	1, 10	∗		-	
2259007	8.1134	0.0173	1, 10	∗	1.5036	0.2436	1, 12
2259049	14.3880	0.0035	1, 10	∗	1.2539	0.2847	1, 12
2259083	18.7899	0.0015	1, 10	∗	0.0457	0.8343	1, 12
2259224	7.6737	0.0394	1, 5	∗	0.3353	0.5742	1, 11
2259319	11.1051	0.0088	1, 9	∗		-	

∗ Indicates statistical significance after Benjamini-Hochberg correction.

Table 8

Results of regressions of the average percent methylation of each allele on the expression of that allele in hypothalamic tissue.

Age Group	Allele	R^2	F-statistic	P-value	df	n
adult	ZAL2-TS	0.0030	0.0305	0.8648	1	12
adult	ZAL2-WS	0.0031	0.0277	0.8714	1	11
adult	ZAL2m-WS	0.0008	0.0074	0.9333	1	11
nestling	ZAL2-TS	0.2300	1.790	0.3127	4	7
nestling	ZAL2-WS	0.2840	0.202	0.6717	4	10
nestling	ZAL2m-WS	0.3240	4.318	0.0923	4	10

Note. Statistics are presented for ANOVAs with polymorphic CpG sites included.

[1]In nestlings, the reported R^2 is the conditional R^2 and the model included a random effect of nest.

Table 9

*Results of regressions of the percent methylation of each TS-*VIP[2] *CpG on the expression of* VIP[2] *in TS adults.*

Position	P-value	R^2	F-statistic	df	n [a]
2258251	0.6519	0.0212	0.2162	1	12
2258330	0.3222	0.0979	1.0846	1	12
2258341	0.0953	0.2533	3.3929	1	12
2258440	0.3125	0.1016	1.1312	1	12
2258539	0.232	0.1393	1.6188	1	12
2258541	0.2411	0.1344	1.5528	1	12
2258572	0.3035	0.1053	1.1765	1	12
2258582	0.2681	0.1209	1.3749	1	12
2258619	0.2919	0.1101	1.2378	1	12
2258627	0.0797	0.2756	3.8048	1	12
2258632	0.112	0.2564	3.1031	1	11
2258636	0.2099	0.3577	2.2272	1	6
2258638 #	0.0266	0.6588	9.6554	1	7
2258647	0.6954	0.0333	0.1721	1	7
2258674	0.257	0.1262	1.4449	1	12
2258707	0.2748	0.1178	1.3351	1	12
2258760	0.3196	0.0988	1.0967	1	12
2258806	0.3564	0.0855	0.9347	1	12
2258830	0.9187	0.0011	0.011	1	12
2258839	0.2274	0.1419	1.6538	1	12
2258841	0.9403	0.0006	0.0059	1	12
2258850	0.687	0.0169	0.1721	1	12
2258852	0.7003	0.0155	0.1569	1	12
2258858	0.5685	0.0336	0.3477	1	12
2258863	0.2294	0.1408	1.6389	1	12
2258869	0.9576	0.0003	0.003	1	12
2258880	0.9266	0.0009	0.0089	1	12
2258884	0.3292	0.0952	1.052	1	12
2258890	0.8388	0.0043	0.0436	1	12
2258893	0.8698	0.0028	0.0283	1	12
2258906	0.4916	0.0485	0.5097	1	12
2258910	0.9268	0.0009	0.0089	1	12
2258928	0.4043	0.0705	0.7583	1	12
2258937	0.6182	0.0258	0.2645	1	12
2258943	0.7453	0.0110	0.1115	1	12
2258947	0.2348	0.1378	1.5983	1	12
2259007	0.4381	0.0612	0.6523	1	12
2259042	0.0841	0.2690	3.6793	1	12
2259049	0.902	0.0016	0.016	1	12
2259083	0.6674	0.0192	0.196	1	12
2259110 #	0.0394	0.4770	6.3841	1	9
2259122	0.2532	0.1813	1.5503	1	9
2259150	0.8337	0.0067	0.0475	1	9
2259153	0.6366	0.0337	0.2438	1	9
2259155	0.9277	0.0013	0.0088	1	9
2259179	0.173	0.2475	2.3017	1	9
2259207	0.2456	0.1866	1.6056	1	9
2259224 #	0.0375	0.4837	6.5579	1	9

2259236	0.4867	0.0838	0.549	1	8
2259241	0.132	0.3361	3.0376	1	8
2259250	0.9252	0.0016	0.0096	1	8
2259256	0.2119	0.2454	1.9514	1	8
2259268	0.5587	0.0600	0.3832	1	8
2259270	0.7286	0.0216	0.1322	1	8
2259278	0.7839	0.0135	0.0822	1	8
2259280	0.6698	0.0324	0.2009	1	8
2259284	0.9916	0.0000	0.0001	1	8
2259293	0.3231	0.1937	1.2009	1	7
2259296	0.1429	0.3213	2.8401	1	8
2259300	0.2964	0.1789	1.3075	1	8
2259303	0.3171	0.1656	1.1904	1	8
2259312	0.0797	0.4253	4.4396	1	8
2259324	0.4016	0.1195	0.8144	1	8
2259338	0.1261	0.4021	3.363	1	7
2259341 ∗	0.0016	0.8835	37.9091	1	7
2259349	0.3008	0.1760	1.2818	1	8
2259392	0.3761	0.1587	0.9432	1	7
2259422	0.0644	0.4602	5.1146	1	8
2259424	0.9902	0.0000	0.0002	1	8

# $p < 0.05$, but not less than the corrected alpha

∗ Indicates statistical significance after Benjamini-Hochberg corrected alpha

[a] Variability in the degrees of freedom was caused by variation in the availability of full-length reads for each bird and thus variation in the coverage at each CpG site, resulting in some missing data at individual CpGs for some birds.

Table 10

*Results of regressions of the percent methylation of each WS-*VIP^2 *CpG on the expression of* VIP^2 *in WS adults.*

Position	P-value	R^2	F-statistic	df	n [a]
2258251	0.2432	0.1477	1.5595	1	11
2258330	0.5078	0.0502	0.4756	1	11
2258341	0.7448	0.0124	0.1127	1	11
2258440	0.2992	0.1188	1.2136	1	11
2258539	0.5264	0.0460	0.4343	1	11
2258541	0.1370	0.2285	2.6650	1	11
2258572	0.5155	0.0484	0.4582	1	11
2258582	0.2087	0.1895	1.8700	1	10
2258619	0.3198	0.1408	1.1467	1	9
2258627	0.3685	0.1361	0.9450	1	8
2258632	0.1332	0.3344	3.0139	1	8
2258636	0.4934	0.0814	0.5316	1	8
2258638	0.7793	0.0141	0.0859	1	8
2258647	0.5389	0.0661	0.4244	1	8
2258674	0.7552	0.0148	0.1052	1	9
2258707	0.8576	0.0038	0.0341	1	11
2258760	0.9272	0.0010	0.0088	1	11
2258806	0.7381	0.0130	0.1190	1	11
2258830	0.6363	0.0259	0.2394	1	11
2258839	0.6862	0.0190	0.1741	1	11
2258841	0.2311	0.1549	1.6494	1	11
2258850	0.4176	0.0742	0.7218	1	11
2258852	0.4038	0.0786	0.7675	1	11
2258858	0.0937	0.2807	3.5125	1	11
2258863	0.7760	0.0095	0.0860	1	11
2258869	0.8313	0.0053	0.0481	1	11
2258880	0.8953	0.0020	0.0183	1	11
2258884	0.4159	0.0748	0.7272	1	11
2258890	0.3479	0.0982	0.9806	1	11
2258893	0.7130	0.0158	0.1441	1	11
2258906	0.6960	0.0178	0.1628	1	11
2258910	0.6252	0.0276	0.2557	1	11
2258928	0.7097	0.0161	0.1476	1	11
2258937	0.8516	0.0041	0.0371	1	11
2258943	0.2882	0.1240	1.2740	1	11
2258947	0.8644	0.0034	0.0309	1	11
2259007	0.8600	0.0036	0.0330	1	11
2259042	0.6114	0.0299	0.2770	1	11
2259049	0.9195	0.0012	0.0108	1	11
2259083	0.8715	0.0031	0.0277	1	11
2259110	0.6493	0.0312	0.2256	1	9
2259122	0.7358	0.0173	0.1233	1	9
2259150	0.2698	0.1702	1.4356	1	9
2259153	0.5518	0.0529	0.3906	1	9
2259155	0.2845	0.1610	1.3433	1	9
2259179	0.5777	0.0464	0.3408	1	9
2259207	0.6960	0.0273	0.1682	1	8
2259224	0.6442	0.0379	0.2361	1	8

2259236	0.4325	0.1055	0.7074	1	8
2259241	0.4181	0.1119	0.7558	1	8
2259250	0.7040	0.0258	0.1589	1	8
2259256 #	0.0321	0.5043	7.1212	1	9
2259268	0.4786	0.0741	0.5602	1	9
2259270	0.9149	0.0018	0.0123	1	9
2259278	0.5921	0.0431	0.3151	1	9
2259280	0.9780	0.0001	0.0008	1	9
2259284	0.9541	0.0005	0.0036	1	9
2259293 #	0.0311	0.5666	7.8425	1	8
2259296	0.9252	0.0019	0.0097	1	7
2259300	0.4014	0.1438	0.8401	1	7
2259303	0.9786	0.0002	0.0008	1	7
2259312	0.8888	0.0043	0.0216	1	7
2259324	0.6784	0.0372	0.1934	1	7
2259338	0.6461	0.0455	0.2383	1	7
2259341	0.5454	0.0775	0.4203	1	7
2259349	0.3799	0.1564	0.9269	1	7
2259392	0.8016	0.0138	0.0702	1	7
2259422 #	0.0261	0.6613	9.7638	1	7
2259424	0.5948	0.0605	0.3223	1	7

# $p < 0.05$, but not less than the corrected alpha

[a] Variability in the degrees of freedom was caused by variation in the availability of full-length reads for each bird and thus variation in the coverage at each CpG site, resulting in some missing data at individual CpGs for some birds.

Table 11

*Results of regressions of the percent methylation of each WS-*VIP^{2m} *CpG on the expression of* VIP^{2m} *in WS adults.*

Position	P-value	R^2	F-statistic	df	n [a]
2258251	0.537	0.0807	0.4388	1	7
2258330	0.6233	0.0519	0.2736	1	7
2258341	0.915	0.0025	0.0126	1	7
2258417	0.8973	0.0037	0.0184	1	7
2258431	0.9364	0.0014	0.007	1	7
2258440	0.4136	0.1371	0.7944	1	7
2258539	0.8313	0.0100	0.0503	1	7
2258541	0.2745	0.2313	1.5048	1	7
2258572	0.2366	0.2655	1.8069	1	7
2258616	0.5708	0.0685	0.3676	1	7
2258619	0.7266	0.0266	0.1368	1	7
2258627	0.7606	0.0203	0.1036	1	7
2258632	0.3562	0.1711	1.0325	1	7
2258636	0.8397	0.0090	0.0454	1	7
2258638	0.5265	0.0847	0.4629	1	7
2258647	0.0617	0.5351	5.7551	1	7
2258674	0.1258	0.4026	3.3702	1	7
2258707	0.8229	0.0059	0.0531	1	11
2258760	0.972	0.0001	0.0013	1	11
2258795	0.3973	0.0807	0.7898	1	11
2258806	0.9557	0.0004	0.0033	1	11
2258830	0.5278	0.0457	0.4313	1	11
2258839	0.8235	0.0058	0.0528	1	11
2258841	0.7794	0.0092	0.0833	1	11
2258850	0.5964	0.0324	0.3014	1	11
2258852	0.2017	0.1741	1.8969	1	11
2258858	0.1198	0.2471	2.9536	1	11
2258863	0.1177	0.2495	2.9917	1	11
2258869	0.7876	0.0085	0.0771	1	11
2258880	0.4061	0.0778	0.7597	1	11
2258884	0.147	0.2187	2.5187	1	11
2258890 #	0.022	0.4589	7.6339	1	11
2258893	0.7487	0.0120	0.1091	1	11
2258906	0.1669	0.2008	2.2607	1	11
2258910	0.155	0.2112	2.4095	1	11
2258928	0.5393	0.0433	0.4071	1	11
2258937	0.5957	0.0325	0.3025	1	11
2258943	0.7854	0.0087	0.0787	1	11
2258947 #	0.0471	0.3699	5.2839	1	11
2259042	0.2541	0.1416	1.4844	1	11
2259049	0.385	0.0848	0.8338	1	11
2259083	0.5512	0.0409	0.3833	1	11
2259110	0.7671	0.0192	0.0978	1	7
2259122	0.8092	0.0128	0.0648	1	7
2259150	0.378	0.1575	0.9348	1	7
2259153	0.2515	0.2515	1.6801	1	7
2259155	0.2204	0.2816	1.9602	1	7
2259179 #	0.0078	0.7867	18.4418	1	7

2259207 #	0.0472	0.5784	6.8591	1	7
2259236	0.4554	0.1157	0.6542	1	7
2259241	0.6782	0.0373	0.1937	1	7
2259250	0.6656	0.0404	0.2105	1	7
2259256	0.4093	0.1395	0.8103	1	7
2259268	0.5983	0.0594	0.3159	1	7
2259270	0.0966	0.4548	4.1706	1	7
2259278	0.926	0.0019	0.0095	1	7
2259280	0.5819	0.0647	0.346	1	7
2259284	0.8309	0.0100	0.0506	1	7
2259293	0.0636	0.5300	5.6379	1	7
2259296	0.8153	0.0120	0.0606	1	7
2259300	0.8323	0.0099	0.0498	1	7
2259303	0.686	0.0354	0.1838	1	7
2259312	0.727	0.0266	0.1364	1	7
2259319 #	0.0084	0.7799	17.7134	1	7
2259324	0.8913	0.0041	0.0207	1	7
2259338	0.6099	0.0709	0.3055	1	6
2259341	0.9911	0.0000	0.0001	1	6
2259349	0.8578	0.0090	0.0365	1	6
2259392	0.2973	0.2638	1.4333	1	6
2259422	0.3124	0.2015	1.2617	1	7
2259424	0.4559	0.1154	0.6525	1	7

# $p < 0.05$, but not less than the corrected alpha

[a] Variability in the degrees of freedom was caused by variation in the availability of full-length reads for each bird and thus variation in the coverage at each CpG site, resulting in some missing data at individual CpGs for some birds.

Table 12

*Results of regressions of the percent methylation of each TS-*VIP[2] *CpG on the expression of* VIP[2] *in TS nestlings.*

Position	P-value	R^2	F-statistic	df	n [a]
2258251	0.3831	0.1545	0.9135	1	7
2258330	0.7552	0.0212	0.1085	1	7
2258341	0.2494	0.2534	1.6975	1	7
2258440	0.8134	0.0122	0.0619	1	7
2258539	0.6765	0.0377	0.1960	1	7
2258541	0.8937	0.0039	0.0198	1	7
2258572	0.6787	0.0372	0.1931	1	7
2258582	0.6095	0.0560	0.2965	1	7
2258619	0.1644	0.3465	2.6506	1	7
2258627	0.8131	0.0123	0.0621	1	7
2258632	0.1314	0.3938	3.2485	1	7
2258636	0.5629	0.0712	0.3834	1	7
2258638	0.7567	0.0210	0.1072	1	7
2258647	0.8285	0.0103	0.0521	1	7
2258674	0.9535	0.0007	0.0038	1	7
2258707	0.6620	0.0413	0.2155	1	7
2258760	0.6152	0.0542	0.2868	1	7
2258806	0.2478	0.2549	1.7109	1	7
2258830	0.8806	0.0050	0.0250	1	7
2258839 ∗	0.0063	0.8026	20.3319	1	7
2258841	0.5696	0.0689	0.3700	1	7
2258850	0.6200	0.0528	0.2789	1	7
2258852	0.4657	0.1108	0.6230	1	7
2258858	0.8132	0.0123	0.0621	1	7
2258863	0.7374	0.0245	0.1257	1	7
2258869	0.5253	0.0852	0.4658	1	7
2258880	0.9226	0.0021	0.0104	1	7
2258884	0.6805	0.0367	0.1907	1	7
2258890	0.3565	0.1710	1.0312	1	7
2258893	0.5783	0.0659	0.3529	1	7
2258906	0.1616	0.3502	2.6952	1	7
2258910	0.4607	0.1131	0.6379	1	7
2258928	0.1655	0.3451	2.6343	1	7
2258937	0.9281	0.0018	0.0090	1	7
2258943	0.4018	0.1437	0.8388	1	7
2258947	0.7472	0.0227	0.1160	1	7
2259007	0.9177	0.0024	0.0118	1	7
2259042	0.6134	0.0548	0.2899	1	7
2259049	0.9917	0.0000	0.0001	1	7
2259083	0.2566	0.2469	1.6394	1	7
2259110	0.7184	0.0283	0.1456	1	7
2259122	0.1776	0.3297	2.4595	1	7
2259150	0.8610	0.0068	0.0340	1	7
2259153 ∗	0.0030	0.8521	28.7983	1	7
2259155	0.8154	0.0120	0.0605	1	7
2259179	0.7256	0.0268	0.1379	1	7
2259207 #	0.0157	0.7203	12.8746	1	7
2259224	0.3337	0.1862	1.1441	1	7

2259236	0.8614	0.0067	0.0338	1	7
2259241	0.5710	0.0684	0.3672	1	7
2259250 ∗	0.0076	0.7884	18.6268	1	7
2259256	0.7108	0.0299	0.1541	1	7
2259268	0.7764	0.0176	0.0898	1	7
2259270	0.0598	0.5402	5.8740	1	7
2259278	0.6759	0.0379	0.1968	1	7
2259280	0.7602	0.0204	0.1039	1	7
2259284	0.5185	0.0879	0.4818	1	7
2259293 #	0.0308	0.6396	8.8736	1	7
2259296	0.2064	0.2963	2.1058	1	7
2259300	0.4447	0.1209	0.6879	1	7
2259303	0.8621	0.0066	0.0335	1	7
2259312	0.8494	0.0079	0.0400	1	7
2259324	0.9837	0.0001	0.0005	1	7
2259338	0.0524	0.5619	6.4133	1	7
2259341 #	0.0239	0.6725	10.2694	1	7
2259349	0.7594	0.0205	0.1046	1	7
2259392	0.3426	0.1801	1.0983	1	7
2259422	0.4373	0.1247	0.7120	1	7
2259424	0.9531	0.0008	0.0038	1	7

# $p < 0.05$, but not less than the corrected alpha

∗ $p <$ Benjamini-Hochberg corrected alpha

[a] Variability in the degrees of freedom was caused by variation in the availability of full-length reads for each bird and thus variation in the coverage at each CpG site, resulting in some missing data at individual CpGs for some birds.

Table 13

*Results of regressions of the percent methylation of each WS-*VIP^2 *CpG on the expression of* VIP^2 *in WS nestlings.*

Position	P-value	R^2	F-statistic	df	n [a]
2258251	0.4137	0.0850	0.7434	1	10
2258330	0.4166	0.0840	0.7337	1	10
2258341	0.9556	0.0004	0.0033	1	10
2258440	0.4207	0.0826	0.7203	1	10
2258539 #	0.0382	0.4343	6.1416	1	10
2258541	0.6035	0.0352	0.2923	1	10
2258572	0.8244	0.0065	0.0526	1	10
2258582	0.8231	0.0066	0.0534	1	10
2258619	0.9306	0.0010	0.0081	1	10
2258627	0.1283	0.2645	2.8763	1	10
2258632	0.8505	0.0047	0.0379	1	10
2258636	0.5237	0.0526	0.4445	1	10
2258638	0.0874	0.3215	3.7913	1	10
2258647	0.7114	0.0181	0.1471	1	10
2258674	0.8447	0.0051	0.0409	1	10
2258707	0.1095	0.2883	3.2401	1	10
2258760	0.0641	0.3655	4.6087	1	10
2258806	0.2409	0.1671	1.6046	1	10
2258830	0.5045	0.0575	0.4883	1	10
2258839	0.6755	0.0230	0.1887	1	10
2258841	0.4186	0.0833	0.7271	1	10
2258850	0.7593	0.0124	0.1005	1	10
2258852	0.4840	0.0631	0.5386	1	10
2258858	0.7154	0.0175	0.1427	1	10
2258863	0.6499	0.0270	0.2222	1	10
2258869	0.8059	0.0080	0.0645	1	10
2258880	0.9710	0.0002	0.0014	1	10
2258884	0.9151	0.0015	0.0121	1	10
2258890	0.0709	0.3515	4.3360	1	10
2258893	0.9520	0.0005	0.0039	1	10
2258906	0.6070	0.0346	0.2866	1	10
2258910	0.8492	0.0048	0.0386	1	10
2258928	0.5028	0.0580	0.4924	1	10
2258937	0.2152	0.1847	1.8121	1	10
2258943	0.2591	0.1557	1.4756	1	10
2258947	0.1250	0.2684	2.9353	1	10
2259007	0.8409	0.0053	0.0430	1	10
2259042	0.1104	0.2872	3.2227	1	10
2259049	0.6097	0.0341	0.2822	1	10
2259083	0.8322	0.0060	0.0479	1	10
2259110	0.4111	0.0984	0.7638	1	9
2259122	0.2233	0.2032	1.7850	1	9
2259150	0.1440	0.2787	2.7049	1	9
2259153	0.9224	0.0015	0.0102	1	9
2259155	0.4337	0.0897	0.6896	1	9
2259179	0.0535	0.4343	5.3736	1	9
2259207	0.0603	0.4170	5.0071	1	9
2259224	0.2080	0.2156	1.9241	1	9

2259236	0.3874	0.1082	0.8494	1	9
2259241	0.0874	0.3604	3.9442	1	9
2259250	0.1258	0.3014	3.0205	1	9
2259256	0.6564	0.0299	0.2157	1	9
2259268	0.5930	0.0429	0.3136	1	9
2259270	0.8934	0.0028	0.0193	1	9
2259278	0.8806	0.0035	0.0243	1	9
2259280	0.7742	0.0125	0.0889	1	9
2259284	0.1050	0.3311	3.4652	1	9
2259293	0.5721	0.0478	0.3512	1	9
2259296	0.6503	0.0310	0.2241	1	9
2259300	0.5168	0.0624	0.4659	1	9
2259303	0.2362	0.1934	1.6789	1	9
2259312	0.7500	0.0154	0.1098	1	9
2259324	0.3015	0.1509	1.2440	1	9
2259338	0.5323	0.0581	0.4314	1	9
2259341	0.9390	0.0009	0.0063	1	9
2259349	0.9424	0.0008	0.0056	1	9
2259392	0.2971	0.1534	1.2688	1	9
2259422	0.3966	0.1043	0.8151	1	9
2259424	0.5552	0.0520	0.3839	1	9

# $p < 0.05$, but not less than the corrected alpha

[a] Variability in the degrees of freedom was caused by variation in the availability of full-length reads for each bird and thus variation in the coverage at each CpG site, resulting in some missing data at individual CpGs for some birds.

Table 14

*Results of regressions of the percent methylation of each WS-*VIP^{2m} *CpG on the expression of* VIP^{2m} *in WS nestlings.*

Position	P-value	R^2	F-statistic	df	n [a]
2258251	0.2271	0.2318	1.8102	1	8
2258330	0.7202	0.0230	0.1411	1	8
2258341	0.1230	0.2709	2.9718	1	10
2258417	0.7672	0.0116	0.0938	1	10
2258431	0.4316	0.0790	0.6859	1	10
2258440	0.5639	0.0433	0.3622	1	10
2258539	0.1115	0.2857	3.1995	1	10
2258541	0.4292	0.0798	0.6934	1	10
2258572	0.7188	0.0171	0.1391	1	10
2258616	0.4393	0.0765	0.6623	1	10
2258619	0.5152	0.0548	0.4636	1	10
2258627	0.2402	0.1675	1.6095	1	10
2258632 #	0.0500	0.3994	5.3189	1	10
2258636	0.7716	0.0111	0.0902	1	10
2258638	0.2650	0.1523	1.4368	1	10
2258647	0.6616	0.0252	0.2064	1	10
2258674	0.0794	0.3353	4.0353	1	10
2258707	0.2517	0.1602	1.5261	1	10
2258760	0.7674	0.0116	0.0936	1	10
2258795	0.8921	0.0024	0.0196	1	10
2258806	0.7747	0.0108	0.0876	1	10
2258830	0.0772	0.3393	4.1091	1	10
2258839	0.8448	0.0051	0.0409	1	10
2258841	0.5500	0.0464	0.3893	1	10
2258850	0.8430	0.0052	0.0419	1	10
2258852	0.7067	0.0187	0.1521	1	10
2258858	0.1774	0.2147	2.1873	1	10
2258863	0.4687	0.0674	0.5786	1	10
2258869	0.2099	0.1885	1.8584	1	10
2258880	0.6996	0.0196	0.1600	1	10
2258884	0.1475	0.2432	2.5705	1	10
2258890	0.4160	0.0842	0.7358	1	10
2258893	0.3368	0.1154	1.0440	1	10
2258906	0.9024	0.0020	0.0160	1	10
2258910	0.5957	0.0367	0.3052	1	10
2258928	0.9809	0.0001	0.0006	1	10
2258937	0.4253	0.0811	0.7056	1	10
2258943	0.1108	0.2866	3.2144	1	10
2258947	0.6215	0.0319	0.2637	1	10
2259042	0.7228	0.0166	0.1351	1	10
2259049	0.8114	0.0075	0.0608	1	10
2259083	0.4915	0.0610	0.5198	1	10
2259110	0.8342	0.0067	0.0472	1	9
2259122	0.5298	0.0587	0.4367	1	9
2259150	0.6385	0.0333	0.2410	1	9
2259153	0.5992	0.0415	0.3028	1	9
2259155	0.2622	0.1752	1.4865	1	9
2259179	0.9428	0.0008	0.0055	1	9

2259207	0.8578	0.0049	0.0345	1	9
2259236	0.7837	0.0115	0.0814	1	9
2259241	0.5454	0.0545	0.4037	1	9
2259250	0.9051	0.0022	0.0153	1	9
2259256	0.8389	0.0063	0.0445	1	9
2259268	0.2679	0.1714	1.4484	1	9
2259270	0.4948	0.0690	0.5184	1	9
2259278	0.0954	0.3464	3.7107	1	9
2259280	0.1438	0.2790	2.7088	1	9
2259284	0.9510	0.0006	0.0041	1	9
2259293	0.4132	0.0975	0.7565	1	9
2259296	0.3741	0.1140	0.9010	1	9
2259300	0.2862	0.1600	1.3330	1	9
2259303	0.0542	0.4325	5.3352	1	9
2259312	0.7817	0.0117	0.0829	1	9
2259319	0.1541	0.2672	2.5527	1	9
2259324	0.3094	0.1464	1.2010	1	9
2259338	0.5178	0.0621	0.4637	1	9
2259341	0.9587	0.0004	0.0029	1	9
2259349	0.9384	0.0011	0.0065	1	8
2259392	0.1085	0.3718	3.5509	1	8
2259422	0.5570	0.0515	0.3803	1	9
2259424	0.0540	0.4331	5.3471	1	9

# $p < 0.05$, but not less than the corrected alpha

[a] Variability in the degrees of freedom was caused by variation in the availability of full-length reads for each bird and thus variation in the coverage at each CpG site, resulting in some missing data at individual CpGs for some birds.

Figures

Figure 1

The white-striped (WS) and tan-striped (TS) morphs in white-throated sparrows. The WS morph (main photo, seen on the branch) is easily distinguished from the TS morph (bottom left) by the bold striping pattern on the crown of the WS morph and the clear, white throat patch. Main photo credit M. R. Prichard, bottom left photo credit B. M. Horton.

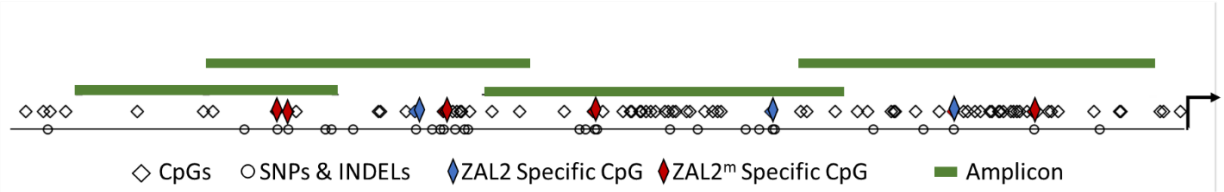

Figure 2

Allelic variation in the *VIP* CRE and the coverage of the amplicons sequenced in this study. CpGs, SNPs, and INDELS within the *cis*-regulatory region are shown. CpGs that are affected by SNPs are represented by colored diamonds; red diamonds indicate CpGs specific to ZAL2^{m} and blue diamonds indicate CpGs specific to ZAL2. The four amplicons that were sequenced in each individual are represented by green bars. The sequence depicted is 1282 total base pairs in length. For information about the primers, see Table 1.

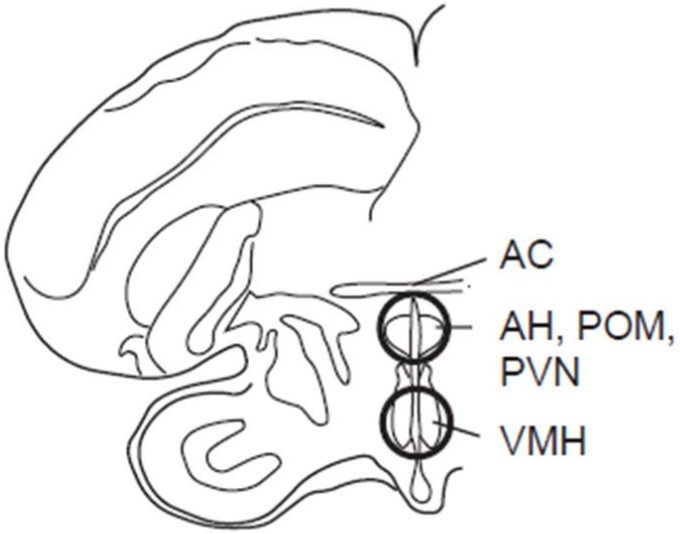

Figure 3

Anatomical locations of neural tissue punches. Samples were taken using a 1mm punch tool on two consecutive 300µm thick sections. Two punches were taken from each section and included the anterior hypothalamus (AH), the caudal portion of the preoptic nucleus of the hypothalamus (POM), the paraventricular nucleus of the hypothalamus (PVN), and the ventromedial hypothalamus (VMH). The anterior commissure (AC) was used as a landmark. The figure is from Zinzow-Kramer et al. (2015).

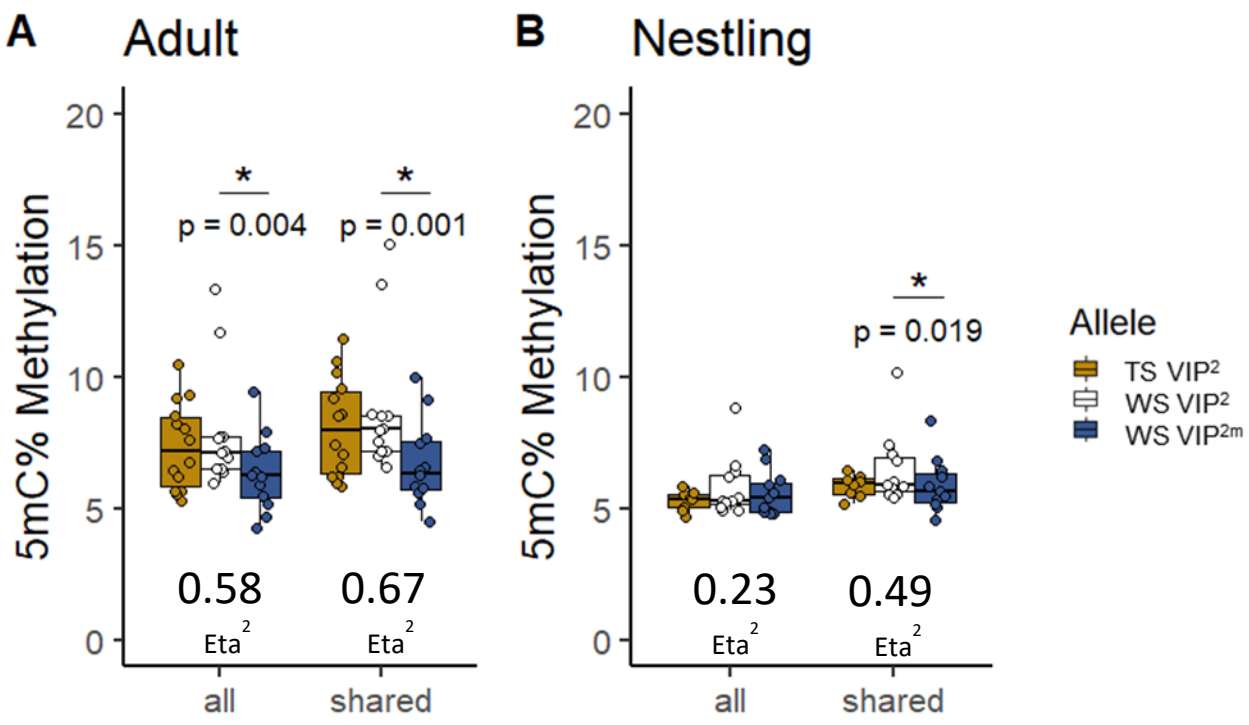

Figure 4

Effects of allele on average percent methylation across the *VIP* CRE. (A) In adults, the VIP^{2m} was significantly less methylated than the VIP^{2} in the WS morph. This effect was stronger when polymorphic CpGs were excluded (see also Tables 2, 3). (B) In nestlings, there was no effect of allele on percent methylation, but a significant effect emerged when polymorphic CpGs were excluded (see also Table 2). WS-*VIP*^{2m} was significantly less methylated than WS-VIP^{2} only when polymorphic CpGs were excluded (Table 3).

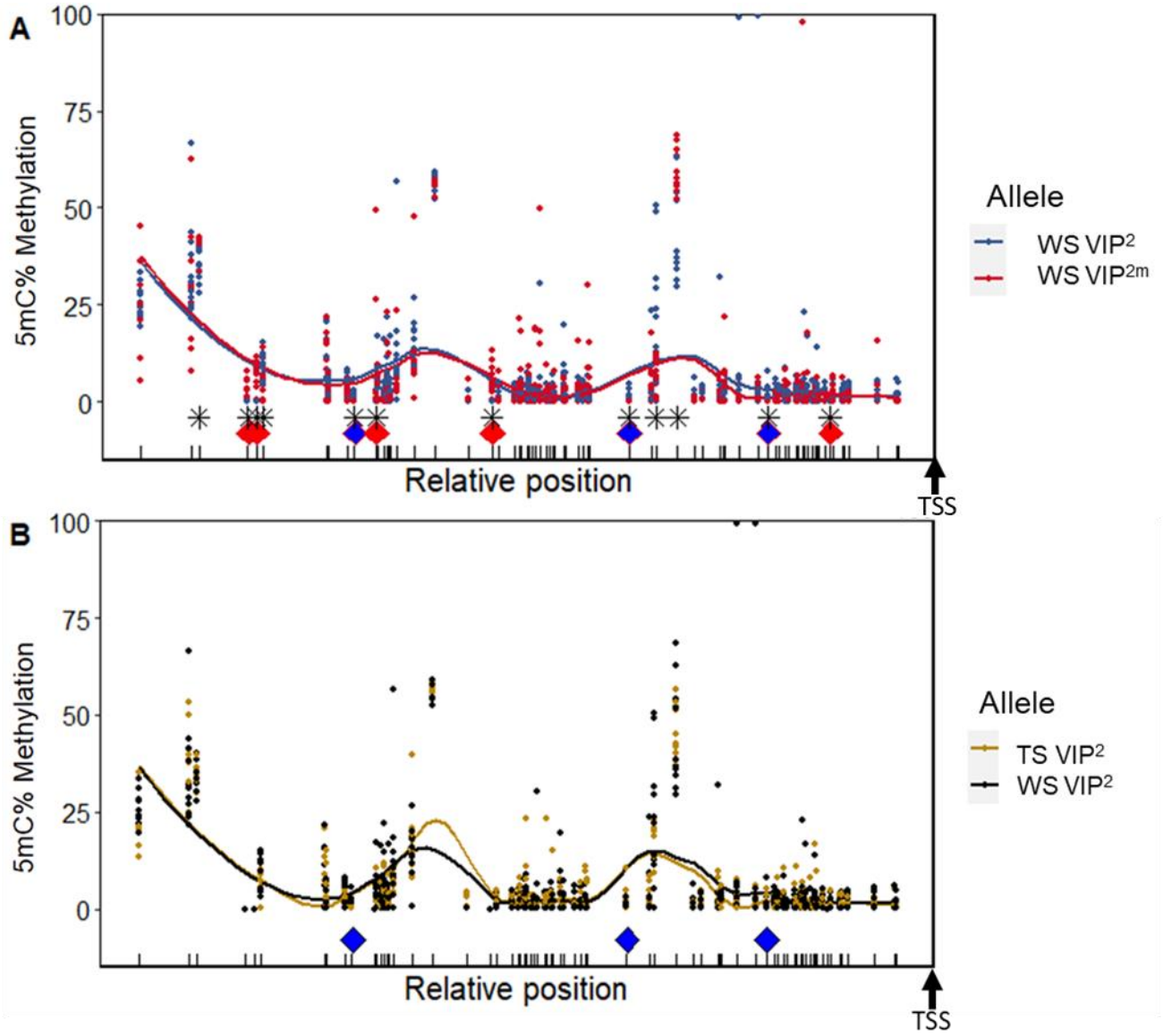

Figure 5

Differences in the percent methylation of each CpG in the *VIP* CRE in adults. In both A and B, the X-axis represents the position of each CpG, indicated by hatch marks, relative to the transcription start site at the far right of the figure. Each dot represents the percent methylation (along the Y-axis) of a CpG in one individual. The solid lines depict a LOESS smooth function indicating how the degree of methylation changes across the region. (A) In WS birds, each red dot indicates the percent methylation of that CpG on ZAL2^{m} in one WS bird. Each blue dot indicates the percent methylation of that CpG on ZAL2 in one WS bird. Differentially

methylated CpGs are indicated with an asterisk directly above the X-axis (see Table 2). Red diamonds above the X-axis indicate ZAL2^{m}-specific CpGs, and blue diamonds indicate ZAL2-specific CpGs. (B) The tan dots indicate the percent methylation for that CpG on ZAL2 in TS birds, and the black dots indicate the percent methylation for that CpG on ZAL2 in WS birds. Blue diamonds indicate the ZAL2-specific CpGs. Only one CpG (black arrow) was differentially methylated both between TS-*VIP*^{2} and WS-*VIP*^{2} and between WS-*VIP*^{2} and WS-*VIP*^{2m} (see also Table 4).

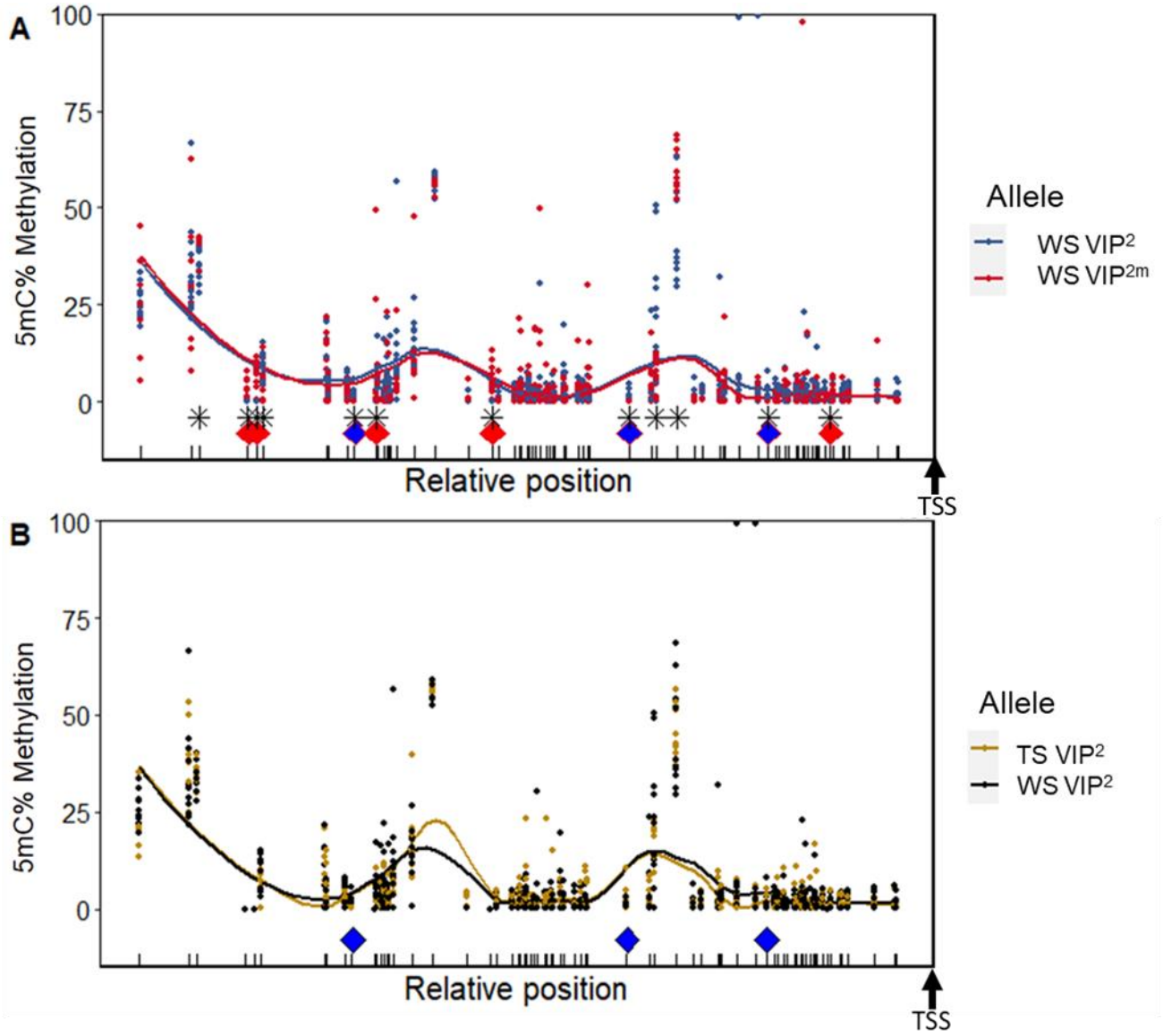

Figure 6

Differences in percent methylation of each CpG in the *VIP* CRE in nestlings. (A) Percent methylation of each CpG on the WS-*VIP*^{2} and WS-*VIP*^{2m} alleles. (B) Percent methylation of each CpG on the WS-*VIP*^{2} and TS-*VIP*^{2} alleles. See Figure 5 for further orientation to this figure and Table 6 and 7 for statistics. All seven of the polymorphic CpGs and four shared CpGs were differentially methylated between WS-*VIP*^{2} and WS-*VIP*^{2m}. There were no differentially methylated CpGs between WS-*VIP*^{2} and TS-*VIP*^{2}.

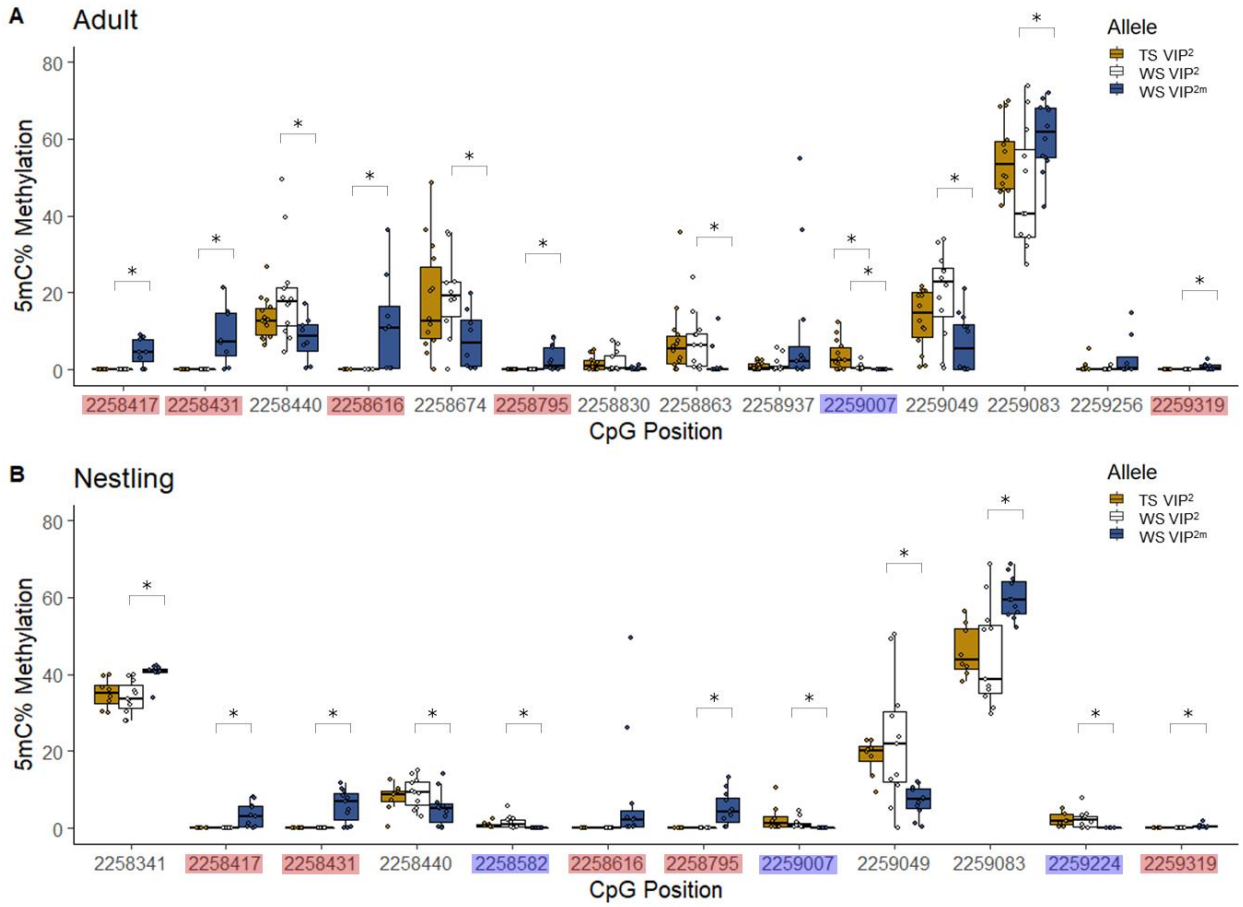

Figure 7

Percent methylation of CpGs at which there was a significant effect of allele. Significant differences in percent methylation, as determined by post-hoc ANOVAs in adults (A; see Table 5) and nestlings (B; see Table 7) are denoted by asterisks. Positions on the X-axis highlighted in red indicate ZAL2^{m}-specific CpGs and blue highlights indicate ZAL2-specific CpGs. For polymorphic sites, the percent methylation was defined as zero on the allele without the site (see Methods). In both age groups, all of the ZAL2^{m}-specific CpGs were significantly methylated (above zero). In contrast, ZAL2-specific CpGs were relatively hypomethylated. In adults, shared CpGs (denoted by lack of highlighting) were less methylated on WS-*VIP*^{2m} than on WS-*VIP*^{2},

with one exception at 2259083. In nestlings, half of the shared CpGs were more methylated on WS-VIP^{2m} and half were more methylated on WS-VIP^{2}.

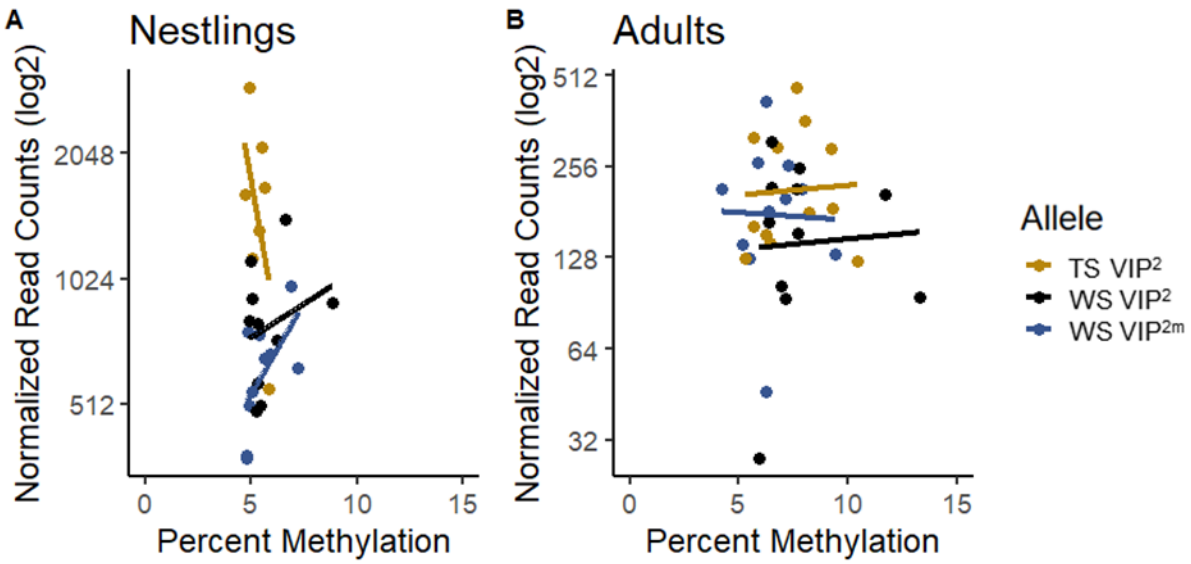

Figure 8

Regressions of percent methylation on *VIP* mRNA read counts. The average percent methylation of each allele of the *VIP* CRE is plotted along the X-axis and the normalized, $\log_2$ transformed read counts of allele-specific *VIP* mRNA are plotted on the Y-axis. The relationship between methylation of an allele and the expression of that allele is shown. None of the relationships in nestlings (A) or adults (B) were statistically significant (see also Table 8).

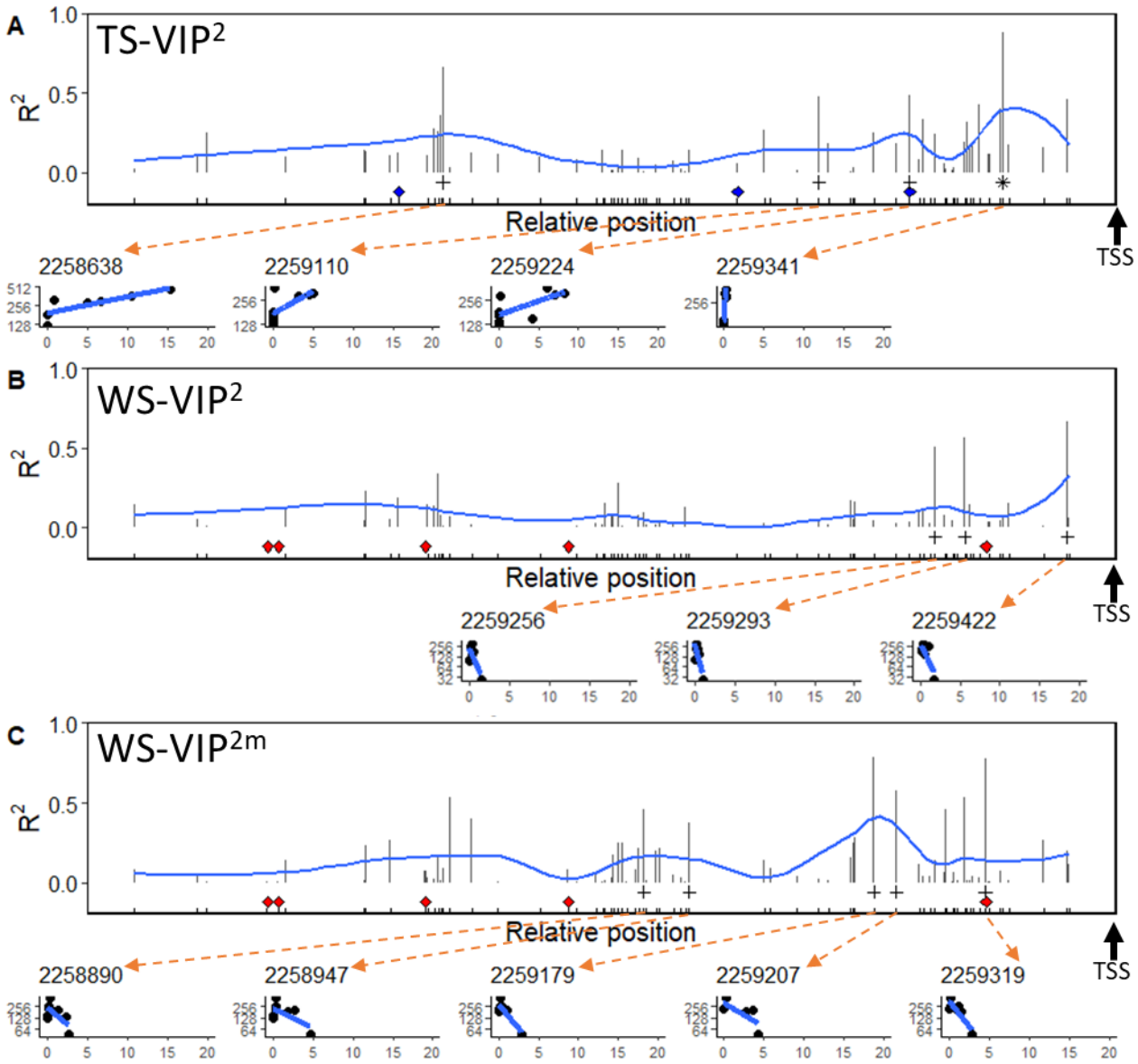

Figure 9

Relationships between percent methylation and expression in adults as a function of position along the *VIP* CRE. R^2 values from the regressions of percent methylation at individual CpGs on the expression of the corresponding allele are plotted for TS-*VIP*^{2} (A), WS-*VIP*^{2} (B), and TS-*VIP*^{2m} (C). In each panel, the magnitude of the R^2 value for each regression is indicated by a vertical black bar at the position of that CpG relative to the transcription start site at the far right

on the X-axis. The blue line in each panel represents a LOESS smooth function over the adjusted R^2 values and shows how the relationship between methylation and expression changes across the region. Red diamonds along the X-axis indicate ZAL2^m-specific CpGs and blue diamonds indicate ZAL2-specific CpGs. Asterisks indicate a significant relationship between the percent methylation of that CpG and expression of the corresponding allele after Benjamini-Hochberg correction. Plus signs indicate relationships with a p-value < 0.05 but that do not survive the correction. The scatterplots show the relationship between percent methylation (X-axis) and expression (Y-axis) for CpGs with p-values that survived the correction (∗) or that were less than 0.05 and did not survive the correction (+). For the full results of each model, see Tables 9-11.

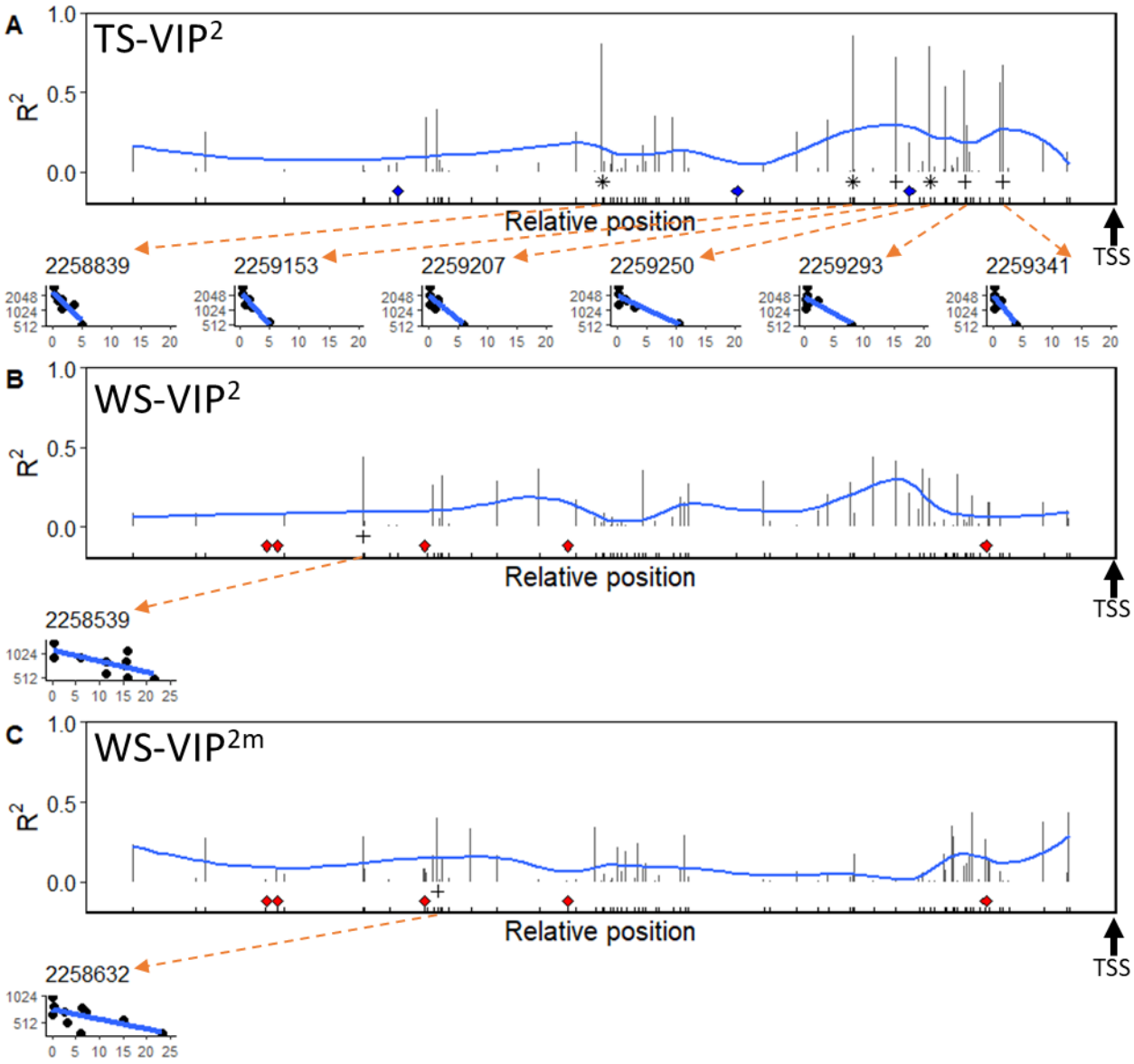

Figure 10

Relationships between percent methylation and expression in nestlings as a function of position along the CRE. R^2 values from the regressions of percent methylation at individual CpG sites on expression of the corresponding allele are plotted for TS-*VIP*^{2} (A), WS-*VIP*^{2} (B), and TS-*VIP*^{2m} (C). For further orientation to this figure, see Figure 9, and for full results of the models, see Tables 12-14.